Title: Dorsomedial striatal neuroinflammation causes excessive goal-directed action control by disrupting homeostatic astrocyte function

Authors and Affiliation:

Arvie Rodriguez Abiero[1,2,3#], Joanne M. Gladding[1#], Jacqueline A. Iredale[4,5], Hannah R. Drury[4,5], Elizabeth E. Manning[4,5], Christopher V. Dayas[4,5], Amolika Dhungana[1,2], Kiruthika Ganesan[1,2,3], Karly Turner[6], Serena Becchi[6,7], Michael D. Kendig[1], Christopher Nolan[6], Bernard Balleine[6], Alessandro Castorina[1], Louise Cole[1], Kelly J. Clemens[8], Laura A. Bradfield[1,2*].

[1]*School of Life Sciences, Faculty of Science, University of Technology Sydney, Sydney, New South Wales 2007, Australia*
[2]*Centre for Neuroscience and Regenerative Medicine, St. Vincent's Centre for Applied Medical Research, St. Vincent's Health Network, Sydney, New South Wales 2010, Australia*
[3]*School of Psychology, Faculty of Science, University of Sydney, Sydney, New South Wales 2006, Australia*
[4]*School of Biomedical Sciences and Pharmacy, College of Health, Medicine and Wellbeing, University of Newcastle, Callaghan, New South Wales 2308, Australia*
[5]*Brain Neuromodulation Research Program, Hunter Medical Research Institute, New Lambton Heights, Sydney, New South Wales 2305, Australia*
[6]*Decision Neuroscience Laboratory, School of Psychology, University of New South Wales, Sydney, New South Wales 2052, Australia*
[7]*Teva Pharmaceuticals, Sydney, New South Wales 2113, Australia*
[8]*School of Psychology, University of New South Wales, Sydney, New South Wales 2052, Australia.*

[#]These authors contributed equally

***Corresponding Author**

Dr. Laura A. Bradfield,

School of Life Sciences, Faculty of Science,

University of Technology Sydney

Building 4, Thomas Street

Ultimo, NSW 2007

laura.bradfield@uts.edu.au

Abstract

Compulsive actions have been confusingly described as reflecting both excessive habitual and excessive goal-directed action control. Here we sought to resolve this contradiction by inducing the neuropathology commonly observed in individuals with compulsive disorders, specifically by causing neuroinflammation in the dorsomedial striatum of rats. We found that this caused rats to be excessively goal-directed, acquiring and maintaining goal-directed actions under conditions that would otherwise produce habits. Immunohistochemical findings suggested that these behaviours were a result of astrocytic proliferation and its effects on neuronal activation. We therefore investigated the role of striatal astrocytes specifically, demonstrating that chemogenetically activating the Gi-pathway in astrocytes altered the firing properties of nearby medium spiny neurons and modulated goal-directed action control. Together, results suggest that striatal neuroinflammation is sufficient to cause excessive goal-directed action control through the dysregulation of astrocyte function suggesting that individuals with striatal neuroinflammation are excessively goal-directed rather than habitual, information that could be used to direct future interventions and/or treatments.

Individuals with compulsive disorders perform actions repetitively, often against their desires and despite negative consequences. This, coupled with observations of aberrant neural activity in the cortico-striatal-thalamic loops that underlie action control, has led to widespread speculation that compulsions arise from a disruption in the balance between goal-directed actions and habits. However, there is debate regarding the proposed direction of this disruption, with some researchers arguing that disorders like substance use disorder (SUD) and obsessive-compulsive disorder (OCD) are best characterised as an overreliance on habits (*1*, *2*), whereas others argue that they reflect excessive goal-directed control (*3*, *4*). Here we address this question in a causal manner by inducing the neuropathological changes associated with disorders of compulsion (including SUD (*5*) and OCD (*6*), but also Parkinson's and Huntington's diseases which often feature compulsivity (*7*, *8*)) and examining the consequences for action selection. Specifically, we first investigated whether regionally-specific striatal neuroinflammation in rats disrupted the balance between goal-directed and habitual action control, then investigated the astrocyte-specific mechanism of that disruption.

The neural circuit of goal-directed and habitual actions has been extensively investigated over the last three decades and has been found to have considerable homology between rodents, primates, and humans (*9*–*11*). Foundational studies (*10*, *11*) revealed that goal-directed and habits actions are controlled by distinct but parallel circuits in the cortico-striatal network, with lesioning or inactivating structures within one circuit producing a shift from one action control system to the other, mirroring the behavioural changes seen in individuals with compulsive disorders. However, the experimental approaches above do not adequately mimic the neural circuit disturbances in individuals with compulsive disorders, who do not exhibit widespread neuronal silencing or death (*14*, *15*), and if they do, it usually

emerges long after symptoms appear (*16*). Therefore, it remains an open question how shifts in action control emerge in such individuals. Interestingly, both post-mortem and neuroimaging studies have reported increased markers of neuroinflammation in the striatum and other regions in such individuals (*6*, *17*). Accordingly, we aimed to mimic this neuropathology in rats so that we could examine the causal consequences of this treatment for goal-directed and habitual action control.

Neuroinflammation was achieved by stereotactically injecting lipopolysaccharide (LPS, 5mg/mL, n=16; Sham controls, n = 14), an endotoxin and neuroinflammatory mimetic, into the striatum. We targeted the posterior dorsomedial striatum (pDMS, Fig. 1B-C) because it is the rodent homologue of the caudate, a region that is known to exhibit abnormal neural activity and elevated neuroinflammatory markers in individuals with substance use disorder (*17*, *18*) and OCD (*14*, *19*, *20*). In rodents, pDMS is considered the neural locus of action control, as it is the only brain region known to be involved in both the learning and performance of goal-directed actions (*12*, *21*). Because we recently showed that neuroinflammation in the hippocampus of mice increased neuronal activation (*22*) we expected a similar effect in the pDMS. We further anticipated that this increased activation would enhance the typical function of pDMS to produce 'excessive' goal-directed action control, which we defined as animals exerting goal-directed control when expected not to. Therefore, for the first series of experiments we adopted experimental parameters under which we expected our Sham animals to show impaired action selection, by feeding them a standard laboratory chow that is relatively high in fat and protein (see supplemental methods and Table 1 for details) on a mild deprivation schedule (approx. 90% of their initial body weight) to induce low levels of hunger and arousal.

We first tested action selection under the guidance of stimuli using the specific Pavlovian-instrumental transfer design shown in Figure 1A. Rats were trained to associate two conditioned stimuli (CSs; a white noise or clicker) with two unique outcomes (sucrose solution or pellet), then to press a left and right lever for the same outcomes. On test, rats were presented with the clicker and noise together with the levers for the first time, but no food. We expected Sham animals to respond equally on each lever regardless of the stimulus presented (due to the mild deprivation conditions) but expected LPS animals to be excessively goal-directed and respond selectively on the lever that had earned the 'same' outcome as the stimulus being presented. That is, the pellet-associated stimulus should elicit presses on the pellet lever more than the sucrose lever, and the sucrose stimulus should elicit presses on the sucrose lever: Same > Different. This prediction was confirmed (Fig. 1D). That is, despite entries into the food magazine and lever press responses not differing between Sham and LPS groups during any phase of acquisition (largest $F(1,28) = 1.085$, $p = 0.362$, Supp. Fig. 1A-C), on test there was a group x transfer interaction, $F(1,28) = 5.710$, $p = 0.024$, which was explained by a significant simple effect of transfer (Same > Different) for group LPS, $F(1,28) = 15.996$, $p = 0.000$, but not Shams (Same = Different), $F < 1$.

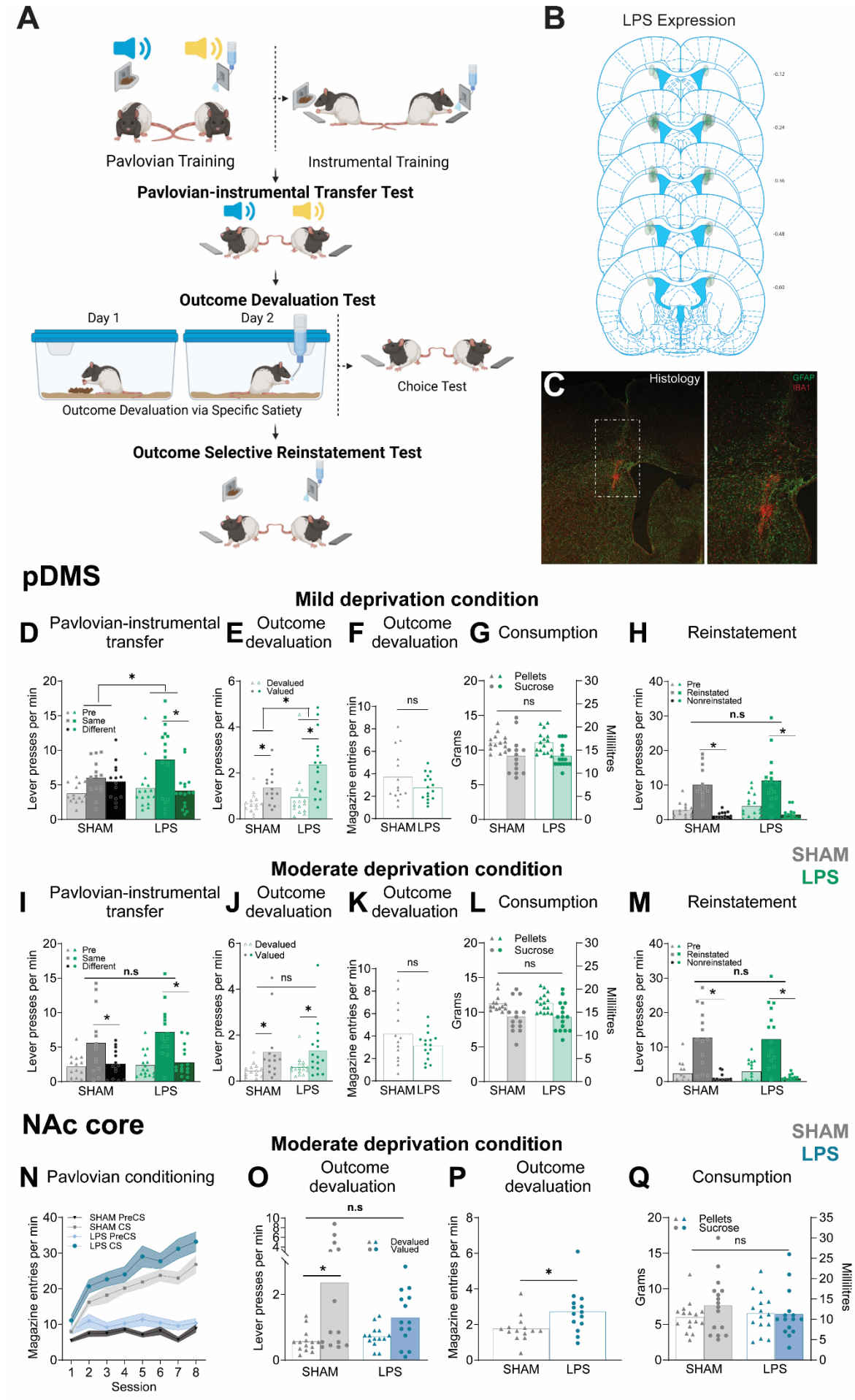
A
Pavlovian Training
Instrumental Training
Pavlovian-instrumental Transfer Test
Outcome Devaluation Test
Day 1
Day 2
Outcome Devaluation via Specific Satiety
Choice Test
Outcome Selective Reinstatement Test
B
LPS Expression
C
Histology
GFAP
IBA1
pDMS
Mild deprivation condition
D Pavlovian-instrumental transfer
E Outcome devaluation
F Outcome devaluation
G Consumption
H Reinstatement
Lever presses per min
Pre
Same
Different
Devalued
Valued
Magazine entries per min
Pellets
Sucrose
Grams
Milliltres
Reinstated
Nonreinstated
SHAM
LPS
ns
n.s
Moderate deprivation condition
I Pavlovian-instrumental transfer
J Outcome devaluation
K Outcome devaluation
L Consumption
M Reinstatement
NAc core
Moderate deprivation condition
N Pavlovian conditioning
O Outcome devaluation
P Outcome devaluation
Q Consumption
SHAM PreCS
SHAM CS
LPS PreCS
LPS CS
Session

Figure 1. Striatal neuroinflammation causes excessive goal-directed action control in a regionally specific manner. (A) Pictorial representation of the experimental procedures for Pavlovian-instrumental transfer, outcome devaluation, and outcome-selective reinstatement, created with *Biorender*. (B) Distribution and locations of the lipopolysaccharide (LPS) injections in the posterior dorsomedial striatum (pDMS) included in the analysis. (C) pDMS image showing LPS placement as labelled with GFAP (glial fibrillary protein) and IBA1 (ionized calcium binding adapator molecule 1), (D-H) Individual data plots and mean lever presses during the (D) Pavlovian-instrumental transfer test, (E-F) outcome devaluation test, (G) consumption, and (H) outcome-selective reinstatement test under mild deprivation conditions following pDMS LPS injections. (I-M) Individual data plots and mean lever presses during the (I) Pavlovian-instrumental transfer test, (J-K) outcome devaluation test, (L) consumption, and (M) outcome-selective reinstatement test under moderate (standard) deprivation conditions following pDMS LPS injections. (N) Magazine entries per min (±SEM) during Pavlovian conditioning. (O-Q) Individual data plots and mean lever presses during the (O-P) outcome devaluation test, and (Q) consumption following NAc core LPS injections. * denotes $p < 0.05$. (pDMS: n = 14 (SHAM), n = 16 (LPS), N = 30; NAc core: n = 14 (SHAM), n = 14 (LPS), N = 28).

Next, rats were tested for goal-directed action control in the absence of stimuli using the outcome devaluation design shown in Figure 1A. Rats were retrained to press the two levers for their distinct outcomes, then given a choice test in which both levers were presented without any outcomes delivered. Immediately prior to this test, we reduced the value of either pellets or sucrose using sensory-specific satiety. If goal-directed, animals should prefer the lever associated with the still-valued outcome and avoid the lever associated with the devalued outcome, demonstrating that their actions were motivated by a) the current value of the outcome, and b) the contingency between the action and outcome: the two criteria of goal-direction (*9*, *23*). Again, due to the mild deprivation conditions we again predicted that the devaluation effect (Valued > Devalued) would be attenuated for group Sham and intact for group LPS. This prediction was confirmed (Fig. 1E) indicated by a group x devaluation interaction, $F(1,28) = 4.878$, $p = 0.035$, composed of a small but significant, simple effect for group Sham, $F(1,28) = 7.445$, $p = 0.011$, and a larger

effect for group LPS, $F(1,28) = 31.060$, $p = 0.000$. This difference was confined to the instrumental response because entries into the food magazine did not differ between groups, $F < 1$ (Fig. 1F) and nor did consumption during pre-feeding, $F < 1$ (Fig. 1G).

Following a day of instrumental retraining, rats were tested for outcome-selective reinstatement as again illustrated in Figure 1A. For this test, responding on each lever was extinguished for 15 min, followed by two unsignalled presentations of each outcome. These presentations typically reinstate responding selectively on the lever that had earned that outcome during training, i.e. sucrose presentations elicit presses on the sucrose lever and pellet presentations on the pellet lever (*24*, *25*). Because selective reinstatement is a measure of action selection that is not goal-directed (*24*), we expected that it would remain unaffected by both the mild deprivation conditions and pDMS neuroinflammation. This was confirmed, as reinstatement was intact (Reinstated > Nonreinstated) for both groups (Fig. 1H) supported by a main effect of reinstatement, $F(1,28) = 67.951$, $p = 0.000$, that did not interact with group, $F < 1$.

To assess whether group differences persisted under moderate deprivation conditions, we switched rats to a lower fat, lower protein laboratory chow and increased the deprivation schedule to maintain rats at approximately 85% of initial body weight (i.e. the standard approach for these kinds of studies, see supplemental methods for details). After brief retraining, we retested the rats using the same transfer, devaluation, and reinstatement tests. This time, performance did not differ between groups on any test. Indeed, on the transfer test both groups responded more on the Same relative to the Different lever: main effect, $F(1,28) = 30.605$, $p = 0.000$ (Figure 1I), interaction with group, $F < 1$. Likewise, on devaluation both groups pressed the Valued more than the Devalued lever; main effect, F

(1,28) = 12.378, p = 0.000 (Figure 1J), which also did not interact with group, F < 1. Finally, reinstatement was again intact for both groups (Reinstated > NonReinstated); main effect (Reinstated > Nonreinstated), F (1,28) = 57.780, p = 0.000 (Figure 1M), and no interaction with group, F < 1.

We next tested whether these effects were regionally specific by injecting LPS into the nucleus accumbens core (NAc core; n=14 LPS, n=14 Sham controls, a ventral striatal region involved in the performance of goal-directed actions (*26*, *27*)). This time, all training and testing occurred under the moderate deprivation/hunger schedule (lower fat/protein chow at 85% bodyweight) because a pilot study revealed that neuroinflammation in the NAc core was unlikely to produce the same increased propensity for goal-directed control. LPS in the NAc core did not affect instrumental responding during any stage of training or test (Supp. Fig. 1G, Fig. 1O,) but did increase the number of entries rats made into the food magazine during Pavlovian conditioning, as revealed by a main effect of group, F (1,25) = 6.962, p = 0.014 (Fig. 1N), and during devaluation testing, as indicated by a group main effect, F (1,26) = 6.02, p = 0.021 (Fig. 1P). Again, this difference was not due to any influence of LPS on feeding or appetite, because outcome consumption during prefeeding did not differ between groups (F < 1, Fig. 1Q).

Pavlovian conditioning and devaluation testing were the two phases of the experiment for which lever pressing was absent (during Pavlovian conditioning) or low (during devaluation testing, due to rats being prefed to satiety). This pattern of results therefore suggests that NAc core neuroinflammation increased the propensity for Pavlovian responding, but that this effect was masked when response competition from lever pressing was present (i.e. lever pressing and magazine entries compete because rats cannot perform

both at the same time). Because an enhanced propensity to respond to Pavlovian cues is also claimed to contribute to compulsive-like tendencies (*28*, *29*), if translatable, these results suggest that differential distributions of neuroinflammation throughout the striatum could be a multifaceted source of compulsivity.

Following confirmation that the effects of pDMS neuroinflammation on goal-directed action are region-specific, we aimed to determine whether it could also produce excessive goal-directed control under moderate deprivation conditions, specifically when using experimental parameters that have been reliably shown to produce habits (Valued = Devalued) (*30*, *31*). To achieve this, we trained a naïve cohort of rats (n=23 LPS, n=18 Sham) to press a single lever for sucrose on an interval schedule whilst being maintained at approximately 85% of their initial body weight on the low fat/low protein chow described. We then administered a progressive ratio test to determine whether pDMS neuroinflammation had altered motivation *per se*, followed by another devaluation test which was performed after half of the animals were subjected to taste aversion training (shown in Fig. 2A). Specifically, the Devalued group received 3 x pairings of sucrose with lithium chloride injections to induce malaise, whereas the Valued group received saline injections. We expected Sham animals to show evidence of habits (Valued = Devalued) and group LPS to remain goal-directed (Valued > Devalued).

Once again, there were no group differences during lever press acquisition, although the LPS group did appear to lever press marginally more than Shams (Fig. 2B), main effect of group $F(1,39) = 3.36$, $p = 0.074$. Importantly, however, the number of action-outcome pairings did not differ between groups, $F < 1$ (Fig. 2C). During progressive ratio testing,

animals with pDMS neuroinflammation took longer than Shams to reach 'breakpoint' (i.e. 5 minutes without responding) despite the number of lever presses required to earn a sucrose

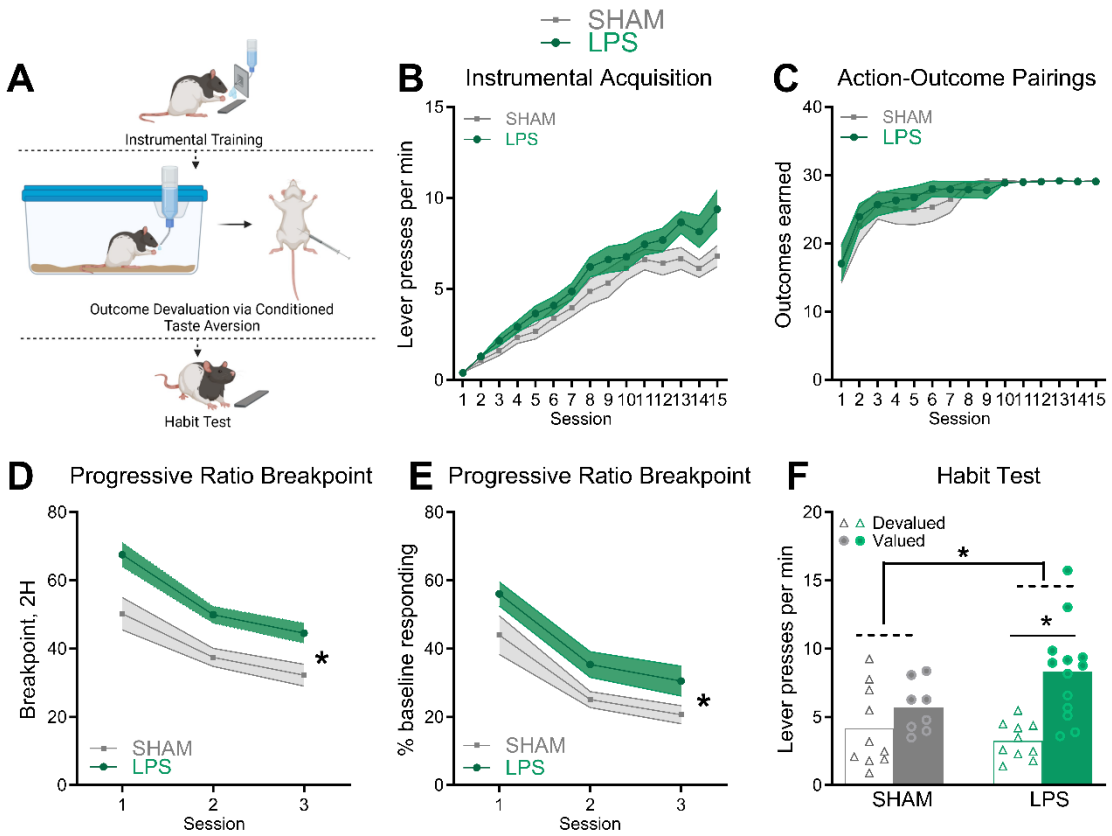

Figure 2. pDMS neuroinflammation prevents the formation of habits. (A) Pictorial representation of the outcome devaluation procedure designed to promote habits created with Biorender. (B) Lever pressing per min (±SEM) during instrumental conditioning and (C) Number of action-outcome pairings (±SEM) during instrumental conditioning, (D) Breakpoint (±SEM) obtained during the 2-h, 3-day Progressive Ratio testing schedule, (E) Lever presses during progressive ratio testing (±SEM) presented as a percentage of baseline responding, (F) Individual data plots and mean lever presses during the outcome devaluation 'habit' test. * denotes $p < 0.05$. (n = 18 (SHAM), n = 23 (LPS), N = 41)

outcome increasing by 5 each time. There was a main effect of group, $F(1,39) = 15.15$, $p = 0.0004$ (Fig. 2D) that remained even after data was corrected for slightly higher lever presses in group LPS at baseline, $F(1,39) = 6.243$, $p = 0.0168$ (Fig. 2E).

As expected, when rats should have been habitual pDMS neuroinflammation produced goal-directed action control (Fig. 2F). There was a group x devaluation interaction, $F(1,37) = 4.373$, $p = 0.043$ consisting of intact devaluation in group LPS (Valued > Devalued), $F(1,37) = 20.198$, $p = 0.000$, and not Shams (Valued = Devalued), $F(1,37) = 1.417$, $p = 0.241$.

These findings show that pDMS neuroinflammation increases motivation *and* causes excessive goal-directed control, which is perhaps unsurprising given the high interdependence of the two processes (*32*). Most importantly, however, they reinforce the notion that pDMS neuroinflammation produces goal-directed control that is excessive, because it prevented the formation of habits which, under non-pathological conditions, are adaptive automated behaviours that allow for more rapid and efficient action execution. Indeed, the inability to form habits has been argued to underscore several cognitive deficits in conditions such as Parkinson's disease (*33*).

Our final aim was to investigate why pDMS neuroinflammation might cause excessive goal-directed control. We turned to the results of our immunohistochemical analyses for clues and found that, although intensity levels, proliferation, and various morphological measures of both the astrocyte marker glial acidic fibrillary protein (GFAP) and microglial marker ionised-calcium binding adaptor molecule (IBA1) were elevated in LPS rats relative to Shams (see Supp. Fig. 3 for full results), only levels of GFAP significantly correlated with action selection on the tests for which performance differed between groups (Fig. 3F-I, although breakpoint responding which also correlated with IBA1 levels, Fig. S3C, suggesting that that more microglia were associated with motivation but not the selectivity of actions). Moreover, and consistent with our findings in hippocampus (*22*), neuronal activation was increased by pDMS neuroinflammation, as evidenced by higher levels of the

activation marker and immediate early gene c-*fos* co-occurring with NeuN in LPS groups relative to Shams (Fig. 3N-O). These levels also significantly correlated selectively with action selection on tests for which group differences were detected (Fig. 3J-M).

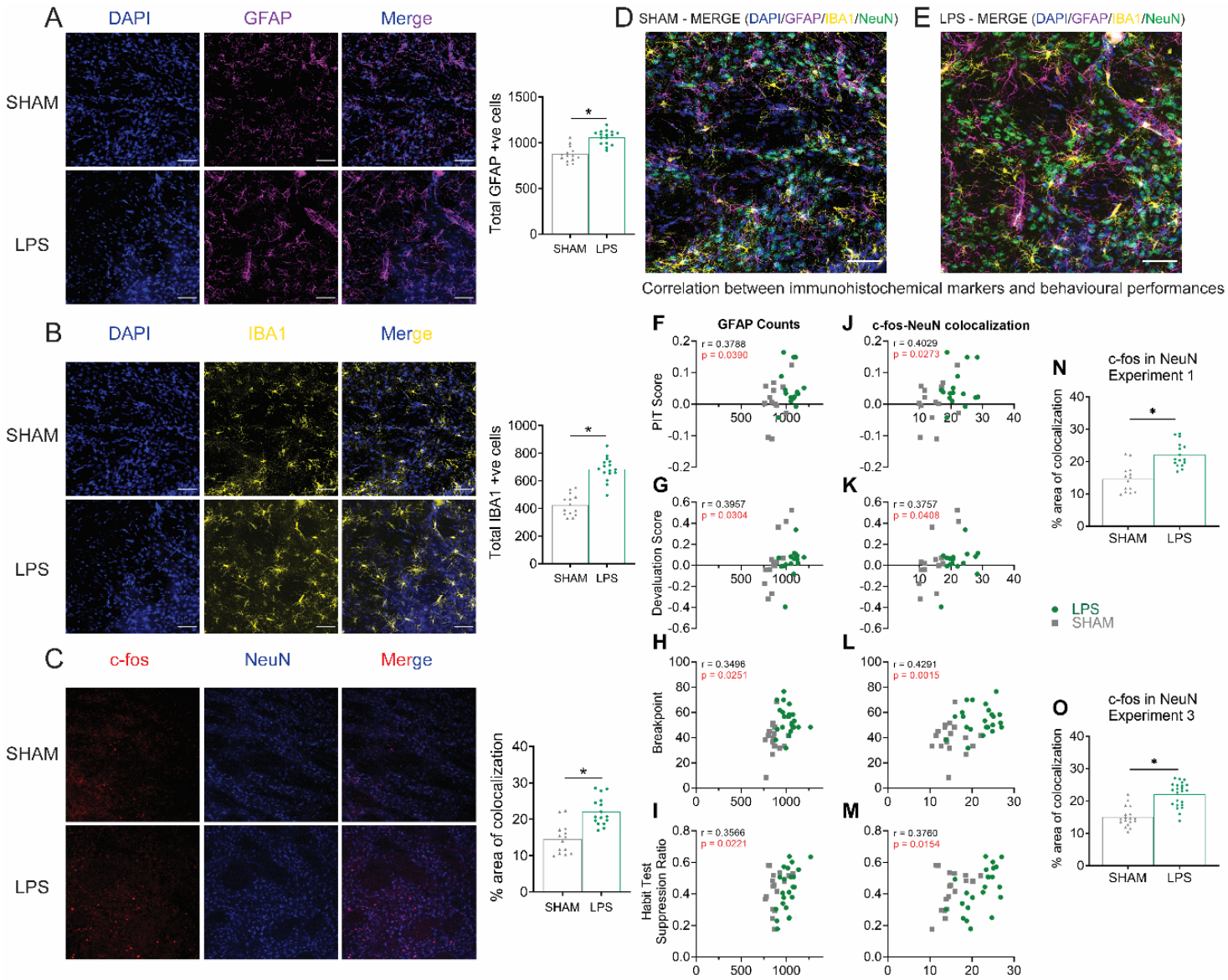

Figure 3. Injections of lipopolysaccharide (LPS) into posterior dorsomedial striatal (pDMS) increased the counts of GFAP, IBA1, and the percentage of c-fos co-localised with NeuN. GFAP and cFos/NeuN co-localisation was correlated with excessive action control. (A-C) Representative images of pDMS from a Sham (top panel) and LPS-injected rat immunostained for DAPI (bottom panel) and (A) GFAP, (B) IBA1, (C) c-*fos*-NeuN, final graphs show individual data points and mean values for quantification of each, (D-E) Representative images of pDMS iummunostained DAPI/GFAP/IBA1/NeuN merged from a Sham (D) and LPS-injected (E) rat, (F-K) Correlations between GFAP, IBA1, and c-fos-NeuN intensity and behavioural performances. * denotes that the $p < 0.05$.

These immunohistochemical results point to pDMS neuroinflammation causing excessive goal-directed action control by altering the interactions between astrocytes and neurons. To gain a more detailed understanding of how this might have occurred, we used *in vitro* whole cell patch clamp electrophysiology to determine whether LPS injections in pDMS altered the firing properties of medium spiny neurons (MSNs). For this study, we once again bilaterally injected LPS (5mg/mL, n = 4) or saline (n = 3) into the pDMS of rats, then removed recorded from the pDMS in acute brain slices 6 weeks after injection. Recordings were first taken at resting membrane potential (RMP, data shown in Supplemental Fig. 4) then repeated while cells were voltage-clamped at -80mV, consistent with the reported *in vivo* RMP of MSNs (*34*). MSNs classification was based on action potential profiles (see supplemental methods for details). LPS MSNs displayed a more depolarised action potential (AP) threshold following a depolarising current steps protocol when voltage-clamped at -80mV ($t_{20.49} = 2.46$, $p = 0.023$, Fig. 4A). No changes were seen for average or instantaneous frequency or interspike interval (Fig. 4B- D). Analysis of the first AP showed changes in the AP profile with increased rise time ($t_{37.34} = 3.21$, $p = 0.003$, Fig. 4E, 4H), and decreased amplitude ($t_{31.31} = 2.72$, $p = 0.011$, Fig. 4F, 4H) in LPS MSNs. Furthermore, LPS MSNs showed a significantly more depolarised afterhyperpolarization (AHP) peak ($t_{28.37} = 3.40$, $p = 0.002$, Fig. 4G, 4I). No changes were seen in rheobase, latency to first spike, half-width or AHP position (data not shown).

Together, these firing patterns suggest that LPS-affected cells were less likely to be activated overall. Taken together these data suggest that LPS produces changes in pDMS circuits that disrupts goal-direct action control; given that goal-directed control requires a precise mix of excitatory and inhibitory responding. For example, performance on an outcome devaluation

test requires animals to respond selectively on the valued lever whilst inhibiting any previously-learned tendency to press the devalued lever.

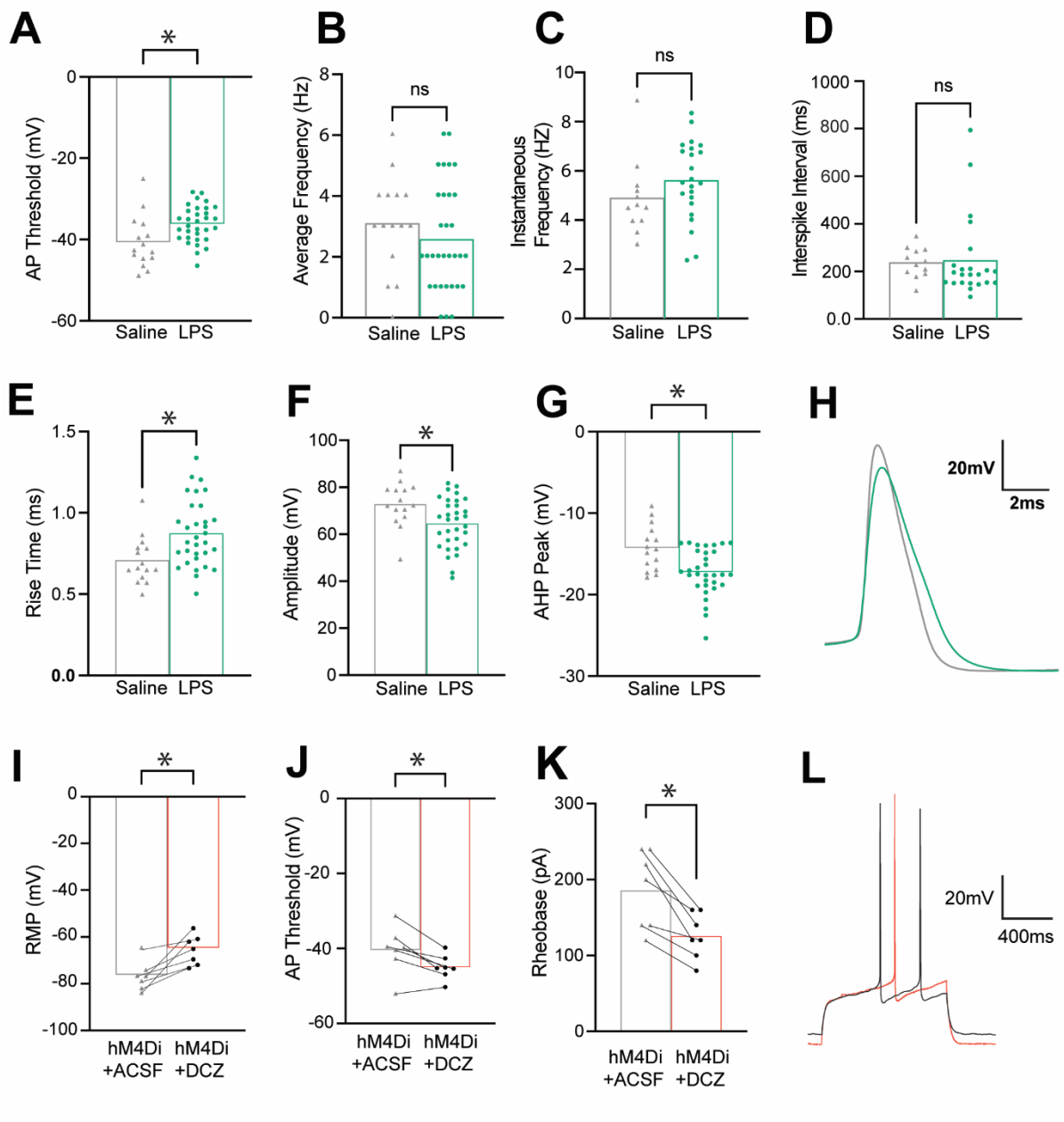

Figure 4. Electrophysiological changes to medium spiny neuron (MSN) action potential (AP) profile and discharge characteristics in pDMS with neuroinflammation or following chemogenetic activation of the Gi-pathway in astrocytes. (A-I) Results of whole-cell patch clamp electrophysiology recordings from MSNs following LPS or sham injections into the pDMS. (A-D) Individual data points showing action potential (AP) threshold for each MSN voltage clamped at -80mV, (B) average frequency of AP discharge, (C) instantaneous frequency, or (D) interspike interval for each MSN. (E-G) Individual data points for changes to AP profile including (E) AP rise time, (F) AP amplitude, and (G) an afterhyperpolarisation

(AHP) peak for each MSN. (H) Example cell average trace show the AP profile characteristics of rise time and amplitude (LPS = green, saline = grey). (I-L) Results of whole-cell patch clamp electrophysiology recordings from MSNs following the application of artificial cerebrospinal fluid (ACSF) then designer receptors exclusively activated by designer drugs (DREADD) agonist deschloroclozapine (DCZ) to astrocytes transfected with hM4Di DREADDs. (I-K) Individual data points showing (I) resting membrane potential (RMP), (J) AP threshold, and (K) rheobase for each MSN. (L) Example cell rheobase traces (ASCF = grey, DCZ = orange). LPS vs saline; LPS at RMP n = 33 cells and at -80 voltage clamp n = 32 cells, from n = 4 animals; saline; n = 15 cells from n = 3 animals. GFAP-HM4Di n = 7 cells from n = 2 animals tested with ACSF then DCZ.

We next turned our attention to astrocytes. Consistent with increased GFAP and c-Fos/Neun expression (Fig. 3) , a previous study that chemogenetically activated hM3Dq designer receptors exclusively activated by designer drugs (DREADDs) (*35*) on astrocytes in DMS found that this led to excessive goal-directed control (albeit in mice and using slightly different behavioural procedures). Thus, we sought to extend these findings by employing a procedure that would reveal information about how pDMS astrocytes might contribute to goal-directed control when in their homeostatic form. Based on evidence that Gi g-protein-coupled receptors (GPCR)s are highly expressed on striatal astrocytes (*36*), and that activating these receptors has been shown to 'correct' a number of Huntington-like (*37*) and compulsion-like (*38*) deficits in mice, we employed astrocyte-specific hM4Di DREADDs to investigate the consequences of activating the Gi pathway on neuronal firing and on action selection.

Although prior studies have investigated the activation of astrocytic Gi-GPCRs in the striatum (*36*, *37*), they have primarily focused on the dorsolateral striatum. Our brief fiber photometry study highlighted the importance of regional specificity to astrocyte function within the striatum (*39*), because it showed that the activation of astrocytic hM4Di-DREADDs in the pDMS produced a different profile of calcium transient activity than it did in the NAc core, as measured by relative increase in fluorescence. Specifically, in pDMS, i.p

injections of the DREADD agonist deschloroclozapine (DCZ) increased the number but not amplitude of calcium peaks (Supp. Fig. 4A), whereas it increased the amplitude of these peaks but not their frequency in the NAc core (Supp. Fig. 4B).

Thus, to establish the effects of astrocytic hM4Di activation on neuronal firing properties, we again employed *in vitro* whole-cell patch clamp electrophysiology. After bilateral injection of GFAP-hM4Di-DREADD into the pDMS, with recordings for each cell (n=7 cells from n=2 animals) taken firstly in artificial cerebrospinal fluid (ACSF) and then repeated following bath application of hM4DI-DREADD agonist DCZ (1µM). Following the application of DCZ, RMP was significantly more depolarised ($t_{6.00} = 4.14$, $p = 0.0118$, Fig. 4J) shifting cells closer to AP threshold. Then, following the same depolarising current steps protocol used in LPS electrophysiology experiments, AP threshold was lower at RMP ($t_{6.00} = 3.57$, $p = 0.012$, Fig. 4K) further narrowing the range between RMP and AP threshold. Rheobase was also significantly reduced following DCZ application ($t_{6.00} = 4.86$, $p = 0.003$ Fig. 4L). No other changes were seen in AP profile (Supp. Fig. 4E-L) or firing properties (data not shown) with DCZ application at either RMP or while cells were voltage-clamped at -80mV.

This profile of MSN firing is in direct contrast to that produced by LPS injection, and also contrasts with the effects of hM3Dq-transfected astrocytes on MSNs observed by Kang et al., (*35*), which reduced EPSPs and IPSPs in both direct and indirect pathway MSNs respectively. Thus, given that both LPS and hM3Dq activation on astrocytes facilitated goal-directed action control whilst producing an opposite profile of neuronal firing, we hypothesised that the activation of Gi receptors on pDMS astrocytes would have the opposite effect and abolish it. Although this prediction may seem counterintuitive, given prior findings that lesioning or otherwise inactivating this structure also abolishes action

control (*12*, *21*), recent findings paint a more nuanced picture of the precise conditions necessary for goal-directed actions (*40*, *41*). In particular, these studies have suggested that spatial-based neuronal ensembles within the striatum must behave in a precise and complementary manner (so-called "behavioural syllables") to produce accurate action selection (*36*). Our electrophysiology results suggest that activating the Gi pathway in pDMS astrocytes disrupts this precision, an effect that would be expected to disrupt the behavioural selectivity necessary for goal-directed action control.

Behavioural experiments employing chemogenetics were conducted under moderate (standard) deprivation conditions. Figure 5A and the bottom left panel of Figure 5B show the representative placements of AAV transfection in the pDMS. The bottom panel of Figure 5C shows a high degree of co-localisation of GFAP and AAV-hM4Di-GFAP-mCherry, and the top panel shows lack of overlap with NeuN, suggesting specificity of transfection for astrocytes. Pavlovian and instrumental training were conducted in the absence of DCZ administrations and proceeded without incident (Supp. Fig. 5A-C, all Fs < 1). Animals did, however, receive vehicle or DCZ injections 25-30 mins prior to each test. Activation of the astrocytic Gi pathway in pDMS prevented transfer, which was impaired (Same = Different) for animals that received both the active virus and DCZ (hM4Di+DCZ; n=12) but was intact (Same > Different) for both vehicle (mCherry or hM4Di+Veh; n=8) and DCZ-only (mCherry+DCZ; n=11) controls (Fig. 5D). There was a group x transfer effect, $F(1,28) = 4.947$, $p = 0.034$, consisting of intact transfer simple effects for groups mCherry+DCZ, $F(1,28) = 5.995$, $p = 0.021$, and hM4Di+Veh, $F(1,28) = 11.731$, $p = 0.002$, but not group hM4Di + DCZ, $F < 1$. It also prevented outcome devaluation, which was intact (Valued > Devalued) for controls, and abolished (Valued = Devalued) for group hM4Di+DCZ (Fig. 5D). The group x devaluation interaction, $F(1,28) = 5.494$, $p = 0.026$, consisted of intact devaluation simple effects for groups hM4Di + Veh,

F(1,28) = 16.464, p = 0.000, and a marginal simple effect for mCherry + DCZ, F(1,28) = 4.063, p = 0.054, and no effect for group hM4Di + DCZ F < 1. Finally, and consistent with our prior LPS findings, performance on selective reinstatement was intact for all groups; main effect (Reinstated > nonReinstated) F(1,28) = 67.965, p = 0.000, interaction F < 1 (Fig. 5E). This latter finding demonstrates that the activation of the Gi pathway in pDMS astrocytes doesn't simply replicate the behavioural results observed following a pDMS lesion or inactivation, which have been shown to abolish reinstatement (*12*) as well as devaluation (*12*, *21*) and transfer (*42*). Rather, these findings demonstrate a distinct role for astrocytes in moderating the neuronal activity that is necessary for intact goal-directed control.

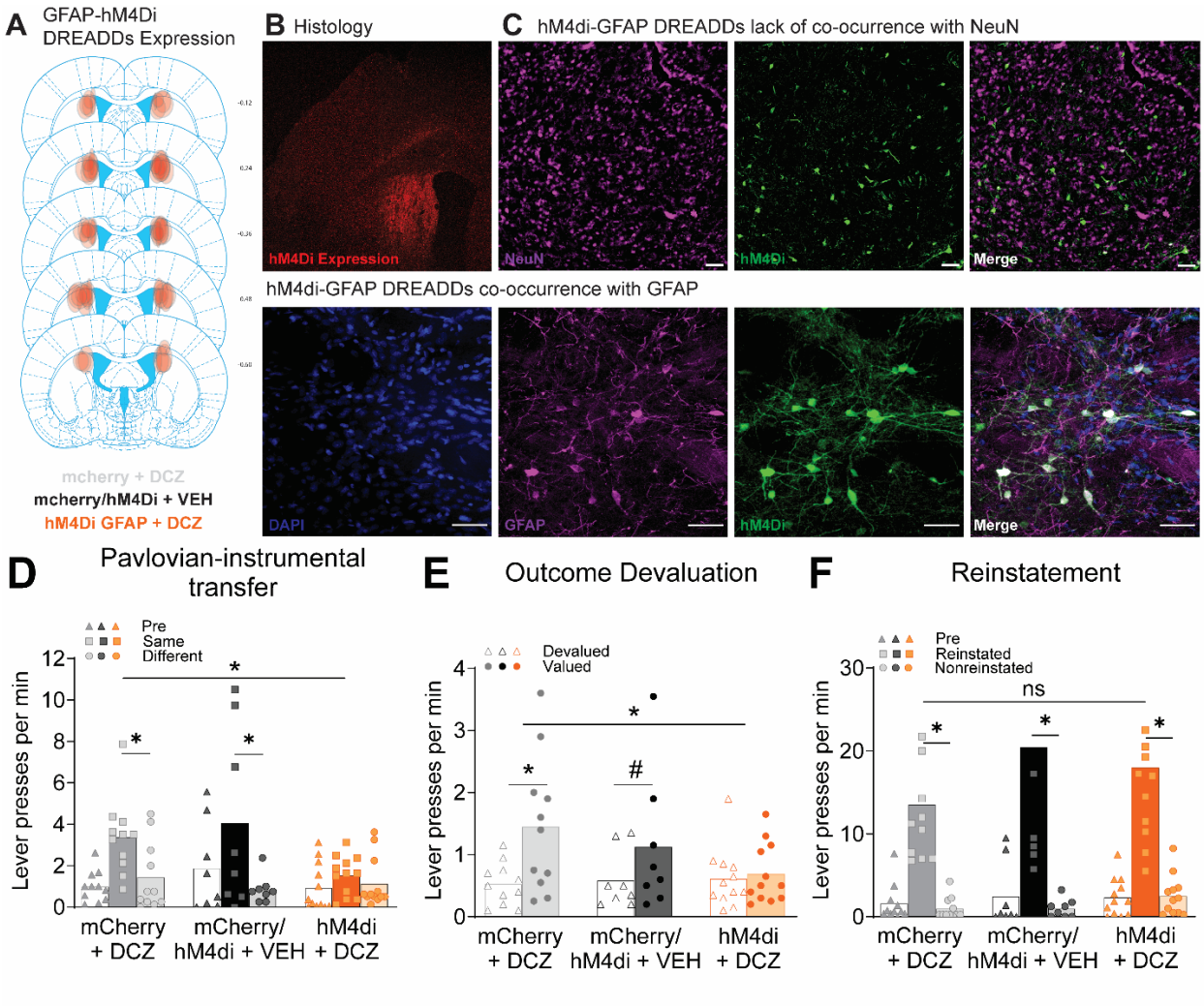

Figure 5. Chemogenetic activation of the Gi-pathway in pDMS astrocytes abolished goal-directed action control. (A) Diagrammatic representation of the distribution and locations of the viral expressions in the pDMS included in the analysis. (B) Histological verification of the GFAP virus expression in pDMS. (C) Representative images showing lack of colocalization with NeuN (top panel) and colocalization of mCherry from GFAP-hM4D-Gi-DREADD virus with the GFAP (bottom panel) scale bars = 45 µm. (D-F) Individual data plots and mean lever presses during the (D) Pavlovian-instrumental transfer test, (E) outcome devaluation test, and (F) outcome-selective reinstatement test. * denotes that the $p < 0.05$, # denotes $p < .055$. (n = 8 (M4/mCherry + VEH), n = 11 (mCherry + DCZ), n = 12 (M4 GFAP + DCZ), N = 31)

Altogether, the results presented here show that pDMS neuroinflammation in the posterior dorsomedial striatum is sufficient to cause excessive goal-directed control, and that it does so because it disrupts the homeostatic function of astrocytes. If translatable, this implies that individuals with neuroinflammation in this brain region, including individuals with compulsive disorders, Parkinson's disease, and Huntington's disease, might struggle to exert adequate control over their actions due to an overreliance on goal-directed control. The specificity of this effect to the pDMS does, however, raise the possibility that individuals with more neuroinflammation in their ventromedial striatum (specifically nucleus accumbens core) might struggle to exert control over their actions due to enhanced responding to Pavlovian cues, rather than effects on goal-directed control per se. It is also possible that individuals may have neuroinflammation in both regions, leading to either type of aberrant action control depending on the relative excitation of each based on the pattern of cortical/thalamic inputs. Overall, then, findings indicate that the alterations to action control experienced by individuals with compulsive disorders cannot be reduced to a single mechanism (*43*), but rather are multifactorial (*44*) and likely operating differently between individuals, or possibly even within the same individual at different times.

Acknowledgements: We thank Tom Burton (UNSW) for his help analysing the fibre photometry data. We thank the technical staff at the Garvan Biological Testing Facility at the Garvan Institute of Medical Research and the technical staff at the Ernst Facility at the University of Technology Sydney, and the Bioresearch Facility Staff at the University of Newcastle for technical support. Figures 1A and 2A were created with BioRender.com.

Funding: This work was supported by the Australian Research Council (ARC) discovery project DP200102445 awarded to L.A.B, and the National Health and Medical Research Council grants GNT2003346 awarded to L.A.B, GNT2028533 awarded to L.A.B. and K.T., GNT1147207 awarded to B.W.B. and C.V.D., and GNT2020768 awarded to C.V.D. and E.M.

Author contributions: A.R.A., J.G., S.B., J.A.I., H.R.D., E.E.M., C.V.D., and L.A.B., conceptualised and designed the research, A.R.A., J.G., J.A.I., H.R.D., A.D., K.G., K.T., and K.C., performed the research (i.e. data curation), A.R.A., J.G., J.A.I., H.R.D., E.E.M., C.V.D., K.T., M.D.K., C.N., L.C., analysed the data, L.A.B., K.T., B.W.B., E.E.M., and C.V.D., acquired the funding, A.R.A., J.G., J.A.I., H.R.D., E.E.M., C.V.D., M.D.K., B.W.B., A.C., and L.A.B. wrote the paper (original draft – A.R.A., J.G., and L.A.B., review and editing - A.R.A., J.G., J.A.I., H.R.D., E.E.M., C.V.D., M.D.K., B.W.B., A.C., and L.A.B.).

Competing Interests: None

Data and materials availability: DOI 10.17605/OSF.IO/297ZU

License information: N/A

References

1. C. M. Gillan, T. W. Robbins, B. J. Sahakian, O. A. Van Den Heuvel, G. Van Wingen, The role of habit in compulsivity. *European Neuropsychopharmacology* **26**, 828–840 (2016).

2. B. J. Everitt, T. W. Robbins, Neural systems of reinforcement for drug addiction: from actions to habits to compulsion. *Nat Neurosci* **8**, 1481–1489 (2005).

3. L. Hogarth, Addiction is driven by excessive goal-directed drug choice under negative affect: translational critique of habit and compulsion theory. *Neuropsychopharmacol.* **45**, 720–735 (2020).

4. S. C. Piantadosi, S. E. Ahmari, Using Optogenetics to Dissect the Neural Circuits Underlying OCD and Related Disorders. *Curr Treat Options Psychiatry* **2**, 297–311 (2015).

5. M. Kohno, J. Link, L. E. Dennis, H. McCready, M. Huckans, W. F. Hoffman, J. M. Loftis, Neuroinflammation in addiction: A review of neuroimaging studies and potential immunotherapies. *Pharmacology Biochemistry and Behavior* **179**, 34–42 (2019).

6. S. Attwells, E. Setiawan, A. A. Wilson, P. M. Rusjan, R. Mizrahi, L. Miler, C. Xu, M. A. Richter, A. Kahn, S. J. Kish, S. Houle, L. Ravindran, J. H. Meyer, Inflammation in the Neurocircuitry of Obsessive-Compulsive Disorder. *JAMA Psychiatry* **74**, 833–840 (2017).

7. M. Alegret, Obsessive-compulsive symptoms in Parkinson's disease. *Journal of Neurology, Neurosurgery & Psychiatry* **70**, 394–396 (2001).

8. K. Dewhurst, J. Oliver, K. L. K. Trick, A. L. McKnight, Neuro-psychiatric Aspects of Huntington's Disease. *Stereotact Funct Neurosurg* **31**, 258–268 (1969).

9. B. W. Balleine, The Meaning of Behavior: Discriminating Reflex and Volition in the Brain. *Neuron* **104**, 47–62 (2019).

10. B. W. Balleine, J. P. O'Doherty, Human and Rodent Homologies in Action Control: Corticostriatal Determinants of Goal-Directed and Habitual Action. *Neuropsychopharmacol* **35**, 48–69 (2010).

11. L. A. Bradfield, B. W. Balleine, "The Learning and Motivational Processes Controlling Goal-Directed Action and Their Neural Bases" in *Decision Neuroscience* (Elsevier, 2017; https://linkinghub.elsevier.com/retrieve/pii/B9780128053089000063), pp. 71–80.

12. H. H. Yin, S. B. Ostlund, B. J. Knowlton, B. W. Balleine, The role of the dorsomedial striatum in instrumental conditioning. *Eur J Neurosci* **22**, 513–523 (2005).

13. H. H. Yin, B. J. Knowlton, B. W. Balleine, Lesions of dorsolateral striatum preserve outcome expectancy but disrupt habit formation in instrumental learning. *Eur J Neurosci* **19**, 181–189 (2004).

14. T. V. Maia, R. E. Cooney, B. S. Peterson, The neural bases of obsessive-compulsive disorder in children and adults. *Dev Psychopathol* **20**, 1251–1283 (2008).

15. V. Pando-Naude, S. Toxto, S. Fernandez-Lozano, C. E. Parsons, S. Alcauter, E. A. Garza-Villarreal, Gray and white matter morphology in substance use disorders: a neuroimaging systematic review and meta-analysis. *Transl Psychiatry* **11**, 29 (2021).

16. S. M. De La Monte, J. J. Kril, Human alcohol-related neuropathology. *Acta Neuropathol* **127**, 71–90 (2014).

17. P. Mews, A. M. Cunningham, J. Scarpa, A. Ramakrishnan, E. M. Hicks, S. Bolnick, S. Garamszegi, L. Shen, D. C. Mash, E. J. Nestler, Convergent abnormalities in striatal gene networks in human cocaine use disorder and mouse cocaine administration models. *Sci. Adv.* **9**, eadd8946 (2023).

18. J. L. Cadet, V. Bisagno, C. M. Milroy, Neuropathology of substance use disorders. *Acta Neuropathol* **127**, 91–107 (2014).

19. S. Saxena, S. L. Rauch, FUNCTIONAL NEUROIMAGING AND THE NEUROANATOMY OF OBSESSIVE-COMPULSIVE DISORDER. *Psychiatric Clinics of North America* **23**, 563–586 (2000).

20. S. C. Piantadosi, E. E. Manning, B. L. Chamberlain, J. Hyde, Z. LaPalombara, N. M. Bannon, J. L. Pierson, V. M. K Namboodiri, S. E. Ahmari, Hyperactivity of indirect pathway-projecting spiny projection neurons promotes compulsive behavior. *Nat Commun* **15**, 4434 (2024).

21. H. H. Yin, B. J. Knowlton, B. W. Balleine, Blockade of NMDA receptors in the dorsomedial striatum prevents action-outcome learning in instrumental conditioning. *Eur J Neurosci* **22**, 505–512 (2005).

22. K. Ganesan, S. Ghorbanpour, W. Kendall, S. T. Broome, J. M. Gladding, A. Dhungana, A. R. Abiero, M. Mahmoudi, A. Castorina, M. D. Kendig, S. Becchi, V. Valova, L. Cole, L. A. Bradfield, Hippocampal neuroinflammation causes sex-specific disruptions in action selection, food approach memories, and neuronal excitation. [Preprint] (2024). https://doi.org/10.1101/2024.05.19.594460.

23. B. W. Balleine, A. Dickinson, Goal-directed instrumental action: contingency and incentive learning and their cortical substrates. *Neuropharmacology* **37**, 407–419 (1998).

24. S. B. Ostlund, B. W. Balleine, Selective reinstatement of instrumental performance depends on the discriminative stimulus properties of the mediating outcome. *Animal Learning & Behavior* **35**, 43–52 (2007).

25. A. R. Abiero, Z. Ali, B. Vissel, L. A. Bradfield, Outcome-selective reinstatement is predominantly context-independent, and associated with c-Fos activation in the posterior dorsomedial striatum. *Neurobiol Learn Mem* **187**, 107556 (2022).

26. L. H. Corbit, J. L. Muir, B. W. Balleine, The Role of the Nucleus Accumbens in Instrumental Conditioning: Evidence of a Functional Dissociation between Accumbens Core and Shell. *J. Neurosci.* **21**, 3251–3260 (2001).

27. G. Hart, L. A. Bradfield, S. Y. Fok, B. Chieng, B. W. Balleine, The Bilateral Prefronto-striatal Pathway Is Necessary for Learning New Goal-Directed Actions. *Curr Biol* **28**, 2218-2229.e7 (2018).

28. T. Robinson, The neural basis of drug craving: An incentive-sensitization theory of addiction. *Brain Research Reviews* **18**, 247–291 (1993).

29. Bradfield, Laura A, Morris, Richard, B. W. Balleine, "Obsessive-compulsive disorder as a failure to integrate goal-directed and habitual action control" in *Obsessive-Compulsive Disorder: Phenomenology, Pathophysiology, and Treatment* (Oxford University Press, 2017), p. 343.

30. C. D. Adams, A. Dickinson, Instrumental Responding following Reinforcer Devaluation. *The Quarterly Journal of Experimental Psychology Section B* **33**, 109–121 (1981).

31. N. W. Lingawi, B. W. Balleine, Amygdala Central Nucleus Interacts with Dorsolateral Striatum to Regulate the Acquisition of Habits. *J. Neurosci.* **32**, 1073–1081 (2012).

32. A. Dickinson, B. Balleine, Motivational control of goal-directed action. *Animal Learning & Behavior* **22**, 1–18 (1994).

33. P. Redgrave, M. Rodriguez, Y. Smith, M. C. Rodriguez-Oroz, S. Lehericy, H. Bergman, Y. Agid, M. R. DeLong, J. A. Obeso, Goal-directed and habitual control in the basal ganglia: implications for Parkinson's disease. *Nat Rev Neurosci* **11**, 760–772 (2010).

34. T. S. Gertler, C. S. Chan, D. J. Surmeier, Dichotomous anatomical properties of adult striatal medium spiny neurons. *J Neurosci* **28**, 10814–10824 (2008).

35. S. Kang, S.-I. Hong, J. Lee, L. Peyton, M. Baker, S. Choi, H. Kim, S.-Y. Chang, D.-S. Choi, Activation of Astrocytes in the Dorsomedial Striatum Facilitates Transition From Habitual to Goal-Directed Reward-Seeking Behavior. *Biol Psychiatry* **88**, 797–808 (2020).

36. B. S. Khakh, Astrocyte-Neuron Interactions in the Striatum: Insights on Identity, Form, and Function. *Trends Neurosci* **42**, 617–630 (2019).

37. X. Yu, J. Nagai, M. Marti-Solano, J. S. Soto, G. Coppola, M. M. Babu, B. S. Khakh, Context-Specific Striatal Astrocyte Molecular Responses Are Phenotypically Exploitable. *Neuron* **108**, 1146-1162.e10 (2020).

38. J. S. Soto, C. Neupane, M. Kaur, V. Pandey, J. A. Wohlschlegel, B. S. Khakh, Astrocyte Gi-GPCR signaling corrects compulsive-like grooming and anxiety-related behaviors in Sapap3 knockout mice. *Neuron*, S0896627324005415 (2024).

39. H. Chai, B. Diaz-Castro, E. Shigetomi, E. Monte, J. C. Octeau, X. Yu, W. Cohn, P. S. Rajendran, T. M. Vondriska, J. P. Whitelegge, G. Coppola, B. S. Khakh, Neural Circuit-Specialized Astrocytes: Transcriptomic, Proteomic, Morphological, and Functional Evidence. *Neuron* **95**, 531-549.e9 (2017).

40. J. Peak, B. Chieng, G. Hart, B. W. Balleine, Striatal direct and indirect pathway neurons differentially control the encoding and updating of goal-directed learning. *eLife* **9**, e58544 (2020).

41. M. Matamales, A. E. McGovern, J. D. Mi, S. B. Mazzone, B. W. Balleine, J. Bertran-Gonzalez, Local D2- to D1-neuron transmodulation updates goal-directed learning in the striatum. *Science* **367**, 549–555 (2020).

42. L. H. Corbit, P. H. Janak, Posterior dorsomedial striatum is critical for both selective instrumental and Pavlovian reward learning. *Eur J Neurosci* **31**, 1312–1321 (2010).

43. Y. Vandaele, S. H. Ahmed, Habit, choice, and addiction. *Neuropsychopharmacol.* **46**, 689–698 (2021).

44. G. P. McNally, P. Jean-Richard-dit-Bressel, E. Z. Millan, A. J. Lawrence, Pathways to the persistence of drug use despite its adverse consequences. *Mol Psychiatry* **28**, 2228–2237 (2023).

45. Hays, W. L., *Statistics for the Social Sciences.* (New York, Holt, Rinehart, & Winston, 1973).

SUPPLEMENTARY MATERIAL

MATERIALS AND METHODS

Experiment 1 and 2: Effects of neuroinflammation in pDMS and NAc core on goal-directed action control

Animals and housing conditions

For behavioural experiments, a total of 158 Long-Evans rats [34 for Experiment 1 (15 male and 19 female), 31 for Experiment 2 (15 male, 16 female), 54 for Experiment 3 (27 male and 27 female), and 42 for Experiment 4 (20 male and 22 female)], weighing 180–350 g, 8-10 weeks of age at the beginning of the experiment were purchased from the Australian Research Centre, Perth, Australia, and were housed in groups of 2-3 in transparent amber plastic boxes located in a temperature- and humidity-controlled room with a 12-h light/dark (07:00–19:00 h light) schedule. Experiments were conducted during the light cycle. Before the experiments, all animals were habituated to the laboratory settings for a week with full access to food and water and environmental enrichment which include plastic tunnel, shreds of paper, and wooden object to gnaw. Throughout the training and actual experiment, animals were maintained at ~85% of their free-feeding body weight by restricting their food intake to 8-14g of their maintenance diet per day. All procedures were approved by the Ethics Committees of the Garvan Institute of Medical Research Sydney (AEC 18.34), and Faculty of Science, University of Technology Sydney (ETH21-6657), and the University of Newcastle (A-2020-018).

Surgery

Animals were anaesthetized with isoflurane (5% induction, 2–3% maintenance) and positioned in a stereotaxic frame (Kopf Instruments). An incision was made into the scalp to expose the skull surface and the incisor bar was adjusted to align bregma and lambda on the same horizontal plane. Small holes were drilled into the skull above the appropriate targeted region and animals received bilateral injections by infusing 1 µl per hemisphere of LPS (5ug/µl) via a 1-µl glass syringe (Hamilton Company) connected to an infusion pump (Pump 11 Elite Nanomite, Harvard Apparatus) into the pDMS (anteroposterior, −0.2mm; mediolateral, ±2.4mm (male), ±2.3mm (female); and dorsoventral, −4.5mm, relative to bregma) and another cohort of animals received LPS injected into their NAc core (anteroposterior, 1.4mm; mediolateral, ±2.2mm; and dorsoventral, −7.5mm, relative to bregma). The infusion was conducted at a rate of 0.15 µl/min, and injectors were left in place for an additional 5 min to ensure adequate diffusion and to minimize LPS spread along the injector tract. The remaining control animals underwent identical procedures but with injection of sterile saline rather than LPS. A nonsteroidal anti-inflammatory/antibiotic agent were administered preoperatively and postoperatively to minimize pain and discomfort. Animals were allowed to recover for 7 days before the onset of any behavioural training.

Apparatus

All behavioural procedures took place in twelve identical sound attenuating operant chambers (Med Associates, Inc.,) and these chambers were located within individual cubicles. The ceiling, back wall, and hinged front door of the operant chambers were made of a clear Plexiglas and the side wall were made of grey aluminium. The floor was made of stainless steel grids. Each chamber was equipped with a recessed food magazine, located at the base of one end wall, through which 20% sucrose-10% polycose solution (0.2 ml) and food pellets (45 mg;

Bio-Serve, Frenchtown, NJ) could be delivered using a syringe pump and pellet dispenser, into separate compartments respectively. Two retractable levers could be inserted individually on the left and right sides of the magazine. An infrared light situated at the magazine opening was used to detect head entries. Illumination was provided by a 3-W, 24-V houselight situated at the top-centred on the left end wall opposite the magazine provided constant illumination, and an electric fan fixed in the shell enclosure provided background noise (≈70 dB) throughout training and testing. The apparatus was controlled, and the data were recorded using Med-PC IV computer software (Med Associates, Inc.). The boxes also contained a white-noise generator, a sonalert that delivered a 3 kHz tone, and a solanoid that, when activated, delivered a 5 Hz clicker stimulus. All stimuli were adjusted to 80 dB in the presence of background noise of 60 dB provided by a ventilation fan. Outcome devaluation procedures took place in transparent plastic tubs that were smaller, but otherwise identical to the cages in which rats were housed.

Food restriction and Chow maintenance

One week following recovery from surgery, animals underwent 3 days of food restriction before the onset of lever press training. During this time animals received 10-14g of chow per day, and their weight was monitored daily to ensure it remained at ~85% of their pre-surgery body weight. For the initial Pavlovian and instrumental training, as well as the first round of testing for sPIT, devaluation, and reinstatement, the chow that rats were maintained on the higher-fat, higher-protein Gordons Specialty Feed (see Table 1). Following reinstatement testing, animals were switched to a lower fat, lower protein Irradiated Specialty Feed's chow (see Table 1) and re-trained and re-tested.

Pavlovian training

For the first 8 days, animals were placed in operant chambers for 60 min during which they received eight 2 min presentations of two conditioned stimuli (CS; white noise or clicker) paired with one of two outcomes (sucrose solution or pellet) presented on a random time schedule around an average of 30 s throughout each CS presentation. Each CS was presented 4 times, with a variable intertrial interval (ITI) that averaged to 5 min. For half the subjects, tone was paired with sucrose and noise with pellets, with the other half receiving the opposite arrangement. Magazine entries throughout the session were recorded and reported for the 2 min prior to each CS presentation (PreCS) and the 2 min during each CS presentation.

Lever press training

Following Pavlovian training, animals were trained to press a left and right lever over 8 days which earned the same sucrose and grain pellet outcomes. Specifically, for half of the animals, the left lever earned pellets and the right lever earned sucrose, and the other half received the opposite arrangement (counterbalanced). Each session lasted for 50 minutes and consisted of two 10 minutes sessions on each lever (i.e., four x 10 minutes sessions in total) separated by a 2.5 minutes time-out period in which the levers were retracted and the houselight was switched off. Animals could earn a maximum of 40 sucrose and 40 pellets deliveries within the session. For the first 2 days, animals were trained on a continuous reinforcement schedule (CRF) in which each lever press produced a single outcome. Animals were then shifted to a random ratio-5 schedule for the next 3 days (i.e. each action delivered an outcome with a probability of 0.2), then to a RR-10 schedule (or a probability of 0.1) for the final 3 days. After 40 sucrose solutions and 40 pellets were delivered or 50 minutes had elapsed, whichever came first, the session was terminated, levers were retracted, and house lights switched off.

Pavlovian Instrumental Transfer (Specific PIT) test

One day after the end of instrumental training, rats were tested for sPIT performance. For this test, responding on both levers was first extinguished for 8 min to reduce baseline performance. Subsequently, each CS was presented four times over the next 40 min in the following order: clicker-noise-noise-clicker-noise-clicker-clicker-noise. Each CS lasted 2 min and had a fixed ITI of 3 min. Magazine entries and lever pressing rates were recorded throughout the session and responses were separated into PreCS and CS periods (2 min each). Lever presses were recorded, but not reinforced.

Outcome Devaluation

One day after sPIT testing, rats were given 1 day of instrumental retraining on RR-10 in the manner previously described. On the following day, animals were given free access to either the pellets (20 g placed in a bowl) or the sucrose solution (100 ml in a drinking bottle) for 1 hr. The amount of pellets and sucrose solution consumed each day was measured. Animals were then placed in the operant chamber for a 10 min choice extinction test. During this test, both levers were extended and lever presses recorded, but no outcomes were delivered. The next day, a second devaluation test was administered with the opposite outcome (i.e. if animals were prefed on pellets the previous day they were now prefed on sucrose, and vice versa). Following pre-freeding animals were again placed into the operant chambers for a second 10 min choice extinction test. All test results are reported as averaged across these two tests.

Outcome Selective Reinstatement Test

After devaluation testing, rats received one day of instrumental retraining on an RR-10 schedule for 1 day. The next day, animals were tested for outcome-selective reinstatement in which rats received a 15 min period of extinction to reduce baseline performance. They then received four reinstatement trials separated by 4 min each as before, and each reinstatement trial consisted of a single free delivery of either the sucrose solution or the grain pellet presented in the following order: sucrose, pellet, pellet, and sucrose. Responding was measured during the 2 min periods immediately before (pre) and after (post) each delivery.

Switching maintenance chow, re-training and re-testing

As noted, I initially used a highly palatable home chow (high-fat/high-protein lab chow) for Experiment 2 which reduced performance in Sham controls. Following training and testing during which animals were given this chow, I switched to a smaller amount (6-8g) of less palatable home chow (lower-fat/lower-protein lab chow) to increase hunger and motivation to lever press for food, with the aim of improving test performance in group Sham. Then I sought to answer whether pDMS neuroinflammation still facilitated goal-directed action when Sham performance was improved.

Following the switch from Gordon's to Specialty feeds chow, rats were given an additional 4 days of Pavlovian training, and an additional 4 days of intrumental training, then tested for performance on sPIT, outcome devaluation, and outcome-selective reinstatement as before.

Tissue preparation

One day after the outcome-selective reinstatement test, animals were sacrificed via CO2 inhalation and perfused transcardially with cold 4% paraformaldehyde in 0.1 M phosphate buffer saline (PBS; pH 7.3-7.5). Brains were rapidly and carefully removed and postfixed in 4%

paraformaldehyde overnight and then placed in 30% sucrose. Brains were sectioned coronally at 40 µm through the pDMS and NAc core defined by Paxinos and Watson (2014) using a cryostat (CM3050S, Leica Microsystems) maintained at approximately -20℃elsius. The sectioned slices were immediately immersed in cryoprotectant solution and stored in the -20°C freezer.

Later, five representative sections from pDMS and NAc core were selected for each rat. Sections were first washed three times (10 minutes per wash) in PBS to remove any exogenous substances. The sections were then incubated in a blocking solution comprising of 3% Bovine Serum Albumin (BSA) + 0.25% TritonX-100 in 1 x PBS for one hour to permeabilize tissue and block any non-specific binding. Sections were then incubated in anti-GFAP mouse primary antibody (1:300, Cell Signalling Technology Catalog #3670), anti-IBA1 rabbit primary antibody (1:500, FUJIFILM Wako Chemicals U.S.A. Corporation), and anti-NeuN chicken primary antibody (1:1000, GeneTex Catalog #GTX00837) diluted in blocking solution for 72 h at 4°C. Sections were then washed 3 times in 1 × PBS and incubated overnight at 4°C in goat anti-mouse AlexaFluor-488 secondary antibody (1:250, ThermoFisher Catalog #A-11001), donkey anti-rabbit AlexaFluor-568 secondary antibody (1:250, ThermoFisher Catalog #A10042), and goat anti-chicken AlexaFluor-647 secondary antibody (1:250, ThermoFisher Catalog #A-21449), followed by a counterstain with 4′,6-diamidino-2-phenylindole (DAPI; Thermo Scientific; 1:1000, diluted in 1x PBS). Finally, every section was mounted onto Superfrost microscope slides (Fisher Scientific) and were coverslipped (Menzel-Glaser) using the mounting agent Vectashield and left to dry overnight in darkness.

Separate brain sections of the pDMS and NAc core were also processed and incubated in anti-c-fos primary antibody (1:500, Synaptic Systems Catalog #226 003) and anti-NeuN chicken

primary antibody (1:500, GeneTex Catalog #GTX00837) diluted in blocking solution for 72 h at 4°C to see how much activation during neuroinflammation. Sections were then washed 3 times in 1 × PBS and incubated overnight at 4°C in donkey anti-rabbit AlexaFluor-568 secondary antibody (1:500, ThermoFisher Catalog #A10042) and goat anti-chicken AlexaFluor-647 secondary antibody (1:500, ThermoFisher Catalog #A-21449), followed by a counterstain with DAPI (Thermo Scientific; 1:1000, diluted in 1x PBS). Sections were mounted and quantified using the same procedures described above.

Imaging and immunofluorescence analysis

For quantification of GFAP, IBA1, NeuN, and c-fos, a single image was taken of the pDMS and NAc core per hemisphere of each slice (6-10 images in total per brain region of each rat) on a Nikon TiE2 microscope using a 10x objective and Leica STELLARIS 20x air objective for representative images.

Microscopy: Images were quantified using imaging software (ImageJ, Fiji Cell Counter), whereby each fluorescent channel was split to isolate and count the cells of interest. Z-stacks were used instead of simply a single image plane. Briefly, the image was adjusted to 8-bit and background subtraction was applied to remove background noise. Thresholding was used to isolate positive stained cells and the threshold for contrast and brightness was adjusted for all images until consistent between images (maximum: 255, minimum: 0). Images were then converted to binary and finally, the Analyze Particles tool was used to quantify the number of cells based on a minimum particle size of 16. ImageJ counted each cell between our parameters and presented it as a “count.” This was followed by intensity measurement, which is represented as Mean grey value (MGV) and background intensity subtracted from the reported MGV. Spatial co-occurrence was measured for c-fos and NeuN only to determine

levels of neuronal activation. Stacked images of each channel were converted into RGB colour images and made composite. The colour threshold was adjusted to select all the red signal (which was the co-occurrence of c-fos and NeuN), and the percentage area of the selected signal was measured and averaged for each brain using ImageJ.

Data and Statistical analysis

Data were collected automatically by Med-PC and uploaded to Microsoft Excel using Med-PC to Excel software. Pavlovian conditioning and lever press acquisition data was analysed using two-way repeated measures ANOVAs controlling the per-family error rate at $\alpha=0.05$. If conditions for sphericity were not met, the Greenhouse-Geisser correction was applied. To allow for a more fine-grained analysis of test data, all data for sPIT, outcome devaluation, and outcome-selective reinstatement were analysed using complex orthogonal contrasts controlling the per-contrast error rate at $\alpha=0.05$ according to the procedure described by Hays (*45*). Acquisition data were expressed as mean ± standard error of the mean (SEM) averaged across counterbalanced conditions. Test data were expressed as individual data points with means. If interactions were detected, follow-up simple effects analyses ($\alpha=0.05$) were calculated to determine the source of the interaction. For immunohistochemical analysis, counts and intensity were compared between LPS and Sham groups using two tailed t-tests and correlated using GraphPad. Test behaviours were correlated with GFAP, IBA1, NeuN, and c-fos expression, as well as c-fos-NeuN intensity using the immunohistochemical results from Figure 3. For correlations with behaviour we used a “PIT score”, a “devaluation score”, or a “reinstatement score” that were calculated in such a way as to ensure that any association detected was not driven by baseline differences in lever press responding *per se*, but rather by the animals selectivity of responding for one or the other levers. For these scores, we first

calculated suppression ratio (SR) scores on each of the levers individually (i.e., the same and different levers for sPIT, the valued and devalued levers for devaluation, and the reinstated and non-reinstated levers for outcome selective reinstatement) according to Equation 1:

$$1)\quad Score = \frac{\text{Lever Press rate on Test}}{\text{Lever Press rate on Test} + \text{Baseline Lever Press Rate}}$$

In this equation, "baseline lever press rate" was taken as the average press rate on each lever across the last two days of training prior to test. We then calculated the PIT score by subtracting the normalised scores on the different lever from the normalised scores on the same lever (i.e. Same – Different), such that a higher score indicated better sPIT performance. Likewise, for devaluation we subtracted the normalised scores on the devalued from those on the valued lever (i.e. Valued – Devalued), such that a higher score indicated better devaluation performance, and did the same thing for reinstatement, this time subtracting scores on the nonreinstated from scores on the reinstated lever (i.e. Reinstated – NonReinstated) such that a high score indicated better reinstatement performance. Each of these scores were then separately correlated with GFAP, IBA1, c-fos-NeuN intensity (correlations with GFAP, IBA1, and c-fos count can be found in Supplemental Figure 3C-D. Values of $p < 0.05$ were considered statistically significant. The statistical software GraphPad Prism, SPSS, and PSY were used to carry out these analyses.

<u>Experiment 3: Effects pDMS neuroinflammation on overtraining-induced habits</u>

Surgery

All surgical procedures were conducted identically to that described for Experiment 1.

Food restriction and Chow maintenance

For this experiment, animals received only 6-8g of the Irradiated Specialty Feeds chow per day to maintain high motivation conditions. They did not receive Gordon's chow at any point.

Apparatus

All Apparatus were as described for Experiments 1 and 2.

Magazine Training

Following recovery from surgery to inject LPS or saline into the pDMS, animals received 3 days of food deprivation and were then given two sessions of magazine training. For these sessions, the house light was turned on at the start of the session and turned off when the session was terminated. No levers were extended. Sucrose solution was delivered at random 60 s intervals for 30 outcomes per session. The session terminated after 45 min or after 30 outcomes had been delivered, whichever came first.

Lever Press Training

Following magazine training, animals then received 8 days of instrumental training (two sessions per day) to press a single lever for sucrose solution delivery. Animals received three sessions of continuous reinforcement, four sessions of random interval of 15 s (RI-15), four sessions of RI-30, and four sessions of RI-60. Right and left lever assignment was counterbalanced across animals. Sessions ended, levers retracted and the houselight terminated when 30 reinforcements were earned or after 60 min, which ever came first.

Progressive ratio test

Following lever press training, animals underwent 2-h of progressive ratio (PR) testing each day for 3 days. A progressive ratio schedule requires the subject to perform an increasing number of lever presses for the next presentation of a reinforcer (Hodos, 1961). For the

current study, the PR was set at n+5. This meant that animals initially received a sucrose reward for a single lever press, then for 5 lever presses, then n+5 lever presses until breakpoint – with breakpoint defined as 5 min of no lever pressing. The number of responses required to obtain each successive delivery of the sucrose reward was collected automatically by Med-PC.

Outcome devaluation

The day after progressive ratio testing, animals were given 2 days of instrumental retraining on an RI-60 schedule in the manner previously described. The following day, the sucrose solution was devalued using conditioned taste aversion method for half of the animals. That is, all animals were given ad libitum access to sucrose solution in clear plastic tubs for 30 min each day for 3 days. Immediately after the 30 mins, half of each type of lesion group received an intraperitoneal injection of lithium chloride (0.15 M LiCl, 20 ml/kg) to induce illness which the rat will associate with the outcome, effectively devaluing it, after which they placed back in their home cages. The remaining rats received 0.9% purified saline injections (20 ml/kg) and these animals comprised the valued groups. In total this manipulation yielded 4 groups: Sham-Valued, Sham-Devalued, LPS-Valued, LPS-Devalued. The amount of sucrose solution consumed each day was measured.

Extinction test

The day following the last day of LiCl pairings, all animals received a 5 min extinction test. The test began with the insertion of the same lever used during training and ended with the retraction of the lever. Lever presses were recorded, and no sucrose reward was delivered.

Tissue Processing and Fluorescent Microscopy

All tissue processing and microscopy were conducted identically to that described for Experiments 1 and 2.

Statistical analysis

Lever press and magazine entry data were collected automatically by Med-PC (version 5) and uploaded directly to Microsoft Excel using Med-PC to Excel software. Lever press acquisition and progressive ratio data were analysed using repeated measures (Group x Session) ANOVA controlling the per-family error rate at $\alpha=0.05$. To allow for a more fine-grained analysis of test data, we used planned, complex orthogonal contrasts controlling the per-contrast error rate at $\alpha=0.05$ for analyzing the outcome devaluation according to the procedure described by Hays (1973). The amount of sucrose consumed was analysed using Three-Way ANOVA repeated measures. If conditions for sphericity were not met, the Greenhouse-Geisser correction was used. Data analysis was conducted in the manner described for Experiment 3.

Patch-clamp electrophysiology

Acute brain slice preparation

To prepare brain slices animals were deeply anesthetised using ketamine injection (100mg/kg, i.p.) and then rapidly decapitated. Following this, brains were rapidly extracted and immersed in ice-cold sucrose substituted artificial cerebrospinal fluid (ACSF) containing (in mM): 236 sucrose, 25 $NaHCO_3$, 11 glucose, 2.5 KCL, 1 NaH2PO4, 1 MgCl2, and 2.5 CaCl2. Coronal slices (300µm) of the pDMS were made using a vibrating microtome (VT1200s, Leica, Nussloch, Germany). Slices were then transferred to an incubation chamber containing

oxygenated ACSF (120mM NaCl substituted for sucrose) and allowed to equilibrate for 1-hour at room temperature (22-24°C) prior to recording.

Patch-clamp electrophysiology

Slices were transferred to a recording chamber and continuously perfused at a rate of 4-6 bath volumes/min with ASCF constantly bubbled with Carbonox (95% O_2, 5% CO_2) to achieve a final pH of 7.3-7.4. All recordings were obtained at room temperature (22-24°C), with neurons visualized using near-infrared differential interference contrast optics (IR-DIC). Recordings were restricted to the pDMS in both LPS and hM4Di-DREADD studies, and taken using patch pipettes (4-8 MW, Harvard Glass) filled with a potassium gluconate based internal solution containing (in mM): 135 $C_6H_{11}KO_7$, 8 NaCl, 2 Mg_2-ATP, 10 HEPES, 0.1 EGTA, and 0.3 Na_3GTP, pH 7.3 (with KOH). Recordings were collected using a Multiclamp 700B amplifier (Molecular Devices, Sunnyvale CA). Signals were sampled at 20kHz, filtered at 10kHz and digitised using an InstraTECH ITC-18 A/D board (HEKA Instruments, Belmore, New York), acquired using Axograph X software (Axograph X, Sydney, Australia). Putative MSN cell selection was based on MSN cell morphology and post-hoc confirmation of MSN delayed firing AP profile, excluding cells without this profile from analysis.

Once whole-cell recording was initiated, series and input resistance were calculated based on the response to a -5 mV voltage step from a holding potential of -70 mV. These measurements were repeated throughout and at the end of all recordings, and data were rejected if this changed by >20 % for an individual cell. AP discharge was investigated in current clamp mode, firstly at RMP, and subsequently voltage clamped at -80mV by injection of current when necessary. Depolarising current steps used to evoke AP discharge were

increased in 20pA increments for a duration of 1 second and features relating to AP profile were extracted from this data. For recordings using hM4Di-DREADD agonist DCZ (1mM) the above recordings were firstly taken in ACSF and then repeated following bath application of DCZ. Data were analysed offline using Axograph X and Igor Pro 9 (Wavemetrics, Portland, OR) software. AP threshold was taken from rheobase response and AP characteristics were extracted from this including latency to rheobase AP rise time, AP amplitude, AP half-width, AHP peak and AHP position. AP discharge properties were then calculated from rheobase +20pA to determine frequency (mean and instantaneous) and interspike interval.

Statistics

Data is presented as mean ± SEM. Unpaired t-tests with Welch's correction were used to compare LPS and sham affected MSN populations. Paired t-tests were used when comparing unaffected and DCZ treated MSNs.

Experiment 4: Chemogenetic activation of Gi-protein-coupled receptors in astrocytes

Chemogenetics

The DREADD agonist deschloroclozapine (DCZ) dihydrochloride (NIMH D-925) was acquired from National Institute of Mental Health (NIMH) through the NIMH Chemical Synthesis and Drug Supply Program. DCZ was diluted with normal saline (SAL) (0.9% w/v NaCl) to a final injectable concentration of 0.1 mg/kg (at a volume of 1ml/kg). DCZ was always handled in dim/low light conditions (i.e. a single lamp in a darkened room) and freshly prepared on the morning of each test day.

Surgery

All surgical procedures were conducted identically to that described for Experiment 1, except that animals received bilateral injections of 1 µl per hemisphere of AAV-GFAP-hM4Di-mCherry (*Addgene*, item ID 50479-AAV5, titer 7×10^{12} vg/mL). The infusion was conducted at a rate of 0.2 µl/min, and injectors were left in place for an additional 5 min to ensure adequate diffusion and to minimize DREADDs spread along the injector tract. The remaining control animals underwent identical procedures but with injection of AAV-GFAP104-mCherry (*Addgene*, item ID 58909-AAV5, titer 1×10^{13} vg/mL) as control group.

Apparatus and Behavioural Procedures

All apparatus and behavioural procedures were conducted identically to that described for Experiment 1, except for outcome devaluation (specific satiety) where animals were given free access to either the pellets or the sucrose solution for 45 mins instead of 1 hr, after which DCZ was administered intraperitoneally (i.p) and rats returned to their home cage for 25-30 min prior to behavioural testing.

Tissue Processing and Fluorescent Microscopy

The extent of the expression was determined using the boundaries defined by Paxinos and Watson (2014). Sections were then stained with Living Colors® DsRed Polyclonal Antibody (1:500, Takara Bio USA, Inc. Catalog #632496) to recognize the mCherry DREADDs expression, anti-GFAP mouse primary antibody (1:300, Cell Signalling Technology Catalog #3670) to check the co-localization, diluted in blocking solution for 72 h at 4°C. Sections were then washed 3 times in 1 × PBS and incubated overnight at 4°C in donkey anti-rabbit AlexaFluor-568 secondary antibody (1:500, ThermoFisher Catalog #A10042), goat anti-mouse AlexaFluor-488 secondary antibody (1:500, ThermoFisher Catalog #A11001), followed by a counterstain with

DAPI (Thermo Scientific; 1:1000, diluted in 1x PBS). Sections were mounted and quantified using procedures identical to those described above.

Statistical analysis

All statsitical analysis was conducted identically as described for Experiment 1.

Tables

	Gordons Specialty Feed	Irradiated Specialty Feed
Protein	23%	19%
Saturated Fat	21.3%	0.78%
Mono-unsaturated Fat	42.9%	2.06%
Poly-unsaturated Fat	30.7%	1.88%
Crude Fibre	5%	5.20%

Table 1. Nutritional information of the lab chow used during the experiment

Measurement	LPS	Saline	Significant Difference
Amplitude (mV)	67.37	71.09	ns (0.1989)
Rise (ms)	**0.8204**	**0.7286**	*** (0.0489)**
Width (ms)	2.424	2.309	ns (0.3305)
AHP Peak (mV)	-17.33	-15.48	ns (0.0577)
AHP Position (ms)	16.85	17.33	ns (0.8014)
AHP Threshold (mV)	-35.79	-37.82	ns (0.1562)
Rheobase (pA)	196.7	222.0	ns (0.4996)
Latency Rheobase (ms)	608.3	621.5	ns (0.8741)
Resting Membrane Potential (mV)	-73.30	-72.81	ns (0.8514)
Instantaneous Frequency (Hz)	**6.052**	**4.760**	*** (0.0359)**
Average Frequency (Hz)	3.091	3.200	ns (0.8142)
Interspike Interval (ms)	**177.8**	**265.0**	*** (0.0300)**

Table 2: Full results for firing properties of medium spiny neurons in posterior dorsomedial striatum injected with 1ul lipopolysaccharide (LPS, 5mg/mL) at resting membrane potential.

Measurement	LPS	Saline	Significant Difference
Amplitude (mV)	**64.54**	**72.80**	*** (0.0105)**
Rise (ms)	**0.8743**	**0.7086**	**** (0.0027)**
Width (ms)	2.552	2.389	ns (0.2822)
AHP Peak (mV)	**-17.24**	**-14.26**	**** (0.0020)**
AHP Position (ms)	17.61	17.95	ns (0.8497)
AHP Threshold (mV)	**-36.16**	**-40.67**	*** (0.0228)**
Rheobase (pA)	256.3	272.7	ns (0.6721)
Latency Rheobase (ms)	524.1	661.4	ns (0.0778)
Instantaneous Frequency (Hz)	6.340	5.422	ns (0.3581)
Average Frequency (Hz)	2.545	3.067	ns (0.3126)
Interspike Interval (ms)	238.6	230.1	ns (0.8289)

Table 3: Full results for firing properties of medium spiny neurons in posterior dorsomedial striatum injected with 1ul lipopolysaccharide (LPS, 5mg/mL) at -80mV.

Measurement	ACSF	DREADDs	Significant Difference
Amplitude (mV)	75.39	75.30	ns (0.9809)
Rise (ms)	0.7501	0.7640	ns (0.8687)
Width (ms)	2.764	3.074	ns (0.3844)
AHP Peak (mV)	-14.95	-12.07	ns (0.0879)
AHP Position (ms)	23.59	22.64	ns (0.5459)
AP Threshold (mV)	**-40.39**	**-45.04**	*** 0.0118**
Rheobase (pA)	**185.7**	**125.7**	**** 0.0028**
Latency Rheobase (ms)	640.5	441.5	ns (0.2462)
Resting Membrane Potential (mV)	**-76.19**	**-64.67**	**** (0.0018)**
Instantaneous Frequency (Hz)	4.762	4.749	ns (0.9910)
Average Frequency (Hz)	3.429	2.429	ns (0.1563)
Interspike Interval (ms)	227.5	259.5	ns (0.5656)

Table 4: Full results for firing properties of medium spiny neurons adjacent to hM4Di-expressing astrocytes in posterior dorsomedial striatum at resting membrane potential.

Measurement	ACSF	DREADDs	Significant Difference
Amplitude (mV)	79.78	79.49	ns (0.9293)
Rise (ms)	0.6602	0.6550	ns (0.8425)
Width (ms)	2.552	2.937	ns (0.1000)
AHP Peak (mV)	-13.77	-11.19	ns (0.4693)
AHP Position (ms)	21.98	19.39	ns (0.1974)
AP Threshold (mV)	-43.85	-48.04	ns (0.3269)
Rheobase (pA)	203.3	220.0	ns (0.4859)
Latency Rheobase (ms)	611.2	604.2	ns (0.9769)
Instantaneous Frequency (Hz)	4.478	3.664	ns (0.3537)
Average Frequency (Hz)	3.400	2.200	ns (0.0705)
Interspike Interval (ms)	245.2	367.8	ns (0.4086)

Table 5: Full results for firing properties of medium spiny neurons adjacent to hM4Di-expressing astrocytes in posterior dorsomedial striatum at -80mV.

Supplemental Figures and Results

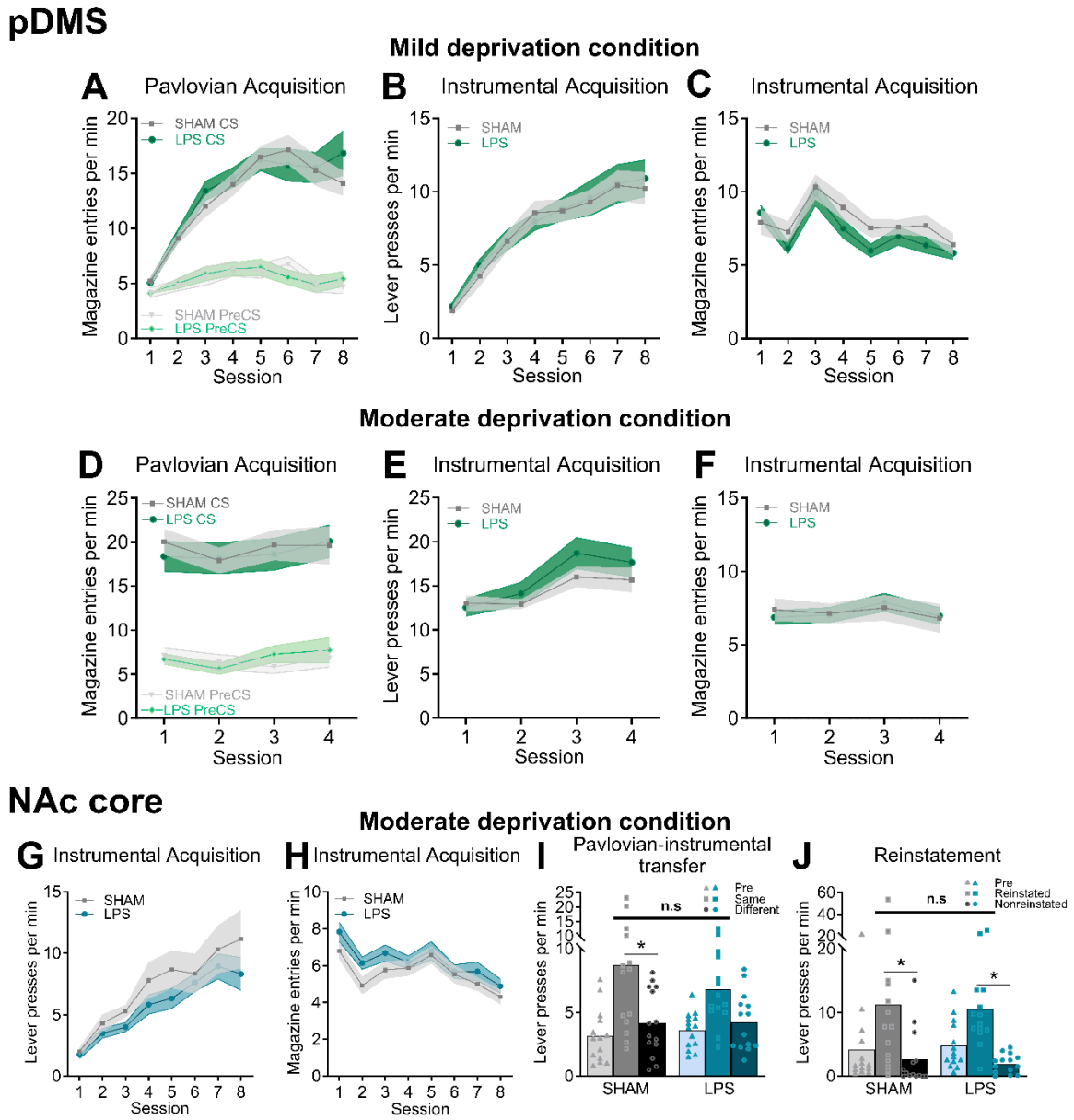

Supplemental Figure 1, relates to Figure 1. Supplemental behaviour results. *There were no significant Sham/LPS differences at any stage of acquisition for pDMS experiment (Experiment 1). (A-C) Acquisition under mild deprivation conditions, (A) Magazine entries per min (±SEM) during Pavlovian conditioning, F (7,196) = 0.669, p = 0.698, for CS x group x session interaction, (B) Lever presses per min (±SEM) during instrumental conditioning, main effect of day F (7,196) = 53.28, p = 0.000, no main effect of group and no day x group interaction, all Fs < 1,(C) Magazine entries per min (±SEM) during instrumental conditioning, main effect of day F (7,196) = 15.282, p = 0.000, no main effect of group and no day x group interaction, all Fs < 1, (D-E) Acquisition under moderate deprivation conditions, (D) Magazine entries per min (±SEM) during Pavlovian conditioning, F (3,84) = 2.15, p = 0.111, for CS x group x session interaction, (E) Lever presses per min (±SEM) during instrumental conditioning, main effect of day F (3,84) = 15.87, p = 0.000, no main effect of group and no day x group interaction, all Fs < 1, (F) Magazine entries per min (±SEM) during instrumental*

conditioning, main effect of day F (3,84) = 2.865, p = 0.041, no main effect of group and no day x group interaction, all Fs < 1. (G-J) Supplemental behavioural results from NAc core neuroinflammation study, there were no significant Sham/LPS differences for this experiment, (G) Lever presses per min (±SEM) during instrumental conditioning, main effect of day F (7,182) = 27.711, p = 0.000, no main effect of group and no day x group interaction, Fs < 1, (H) Magazine entries per min (±SEM) during instrumental conditioning, main effect of day F (7,182) = 9.692, p = 0.000, no main effect of group and no day x group interaction, Fs < 1, (I) Individual data points and mean magazine entries per min during Pavlovian instrumental transfer testing, a main effect of sPIT, F (1,26) = 14.349, p = .001, that did not interact with the group, F (1,26) = 1.118, p = 0.30. A significant simple effect for the Sham group (Same > Different), F (1,26) = 11.739, p = 0.002, but no such effect (or a marginal simple effect) for the LPS group (Same = Different), F (1,26) = 3.728, p = 0 .064, (J) Individual data points and mean magazine entries per min during outcome selective reinstatement testing, a main effect of reinstatement (Reinstated > Nonreinstated) F (1,26) = 19.278, p = 0.000, which did not interact with any group differences, all Fs < 1. denotes p < 0.05.*

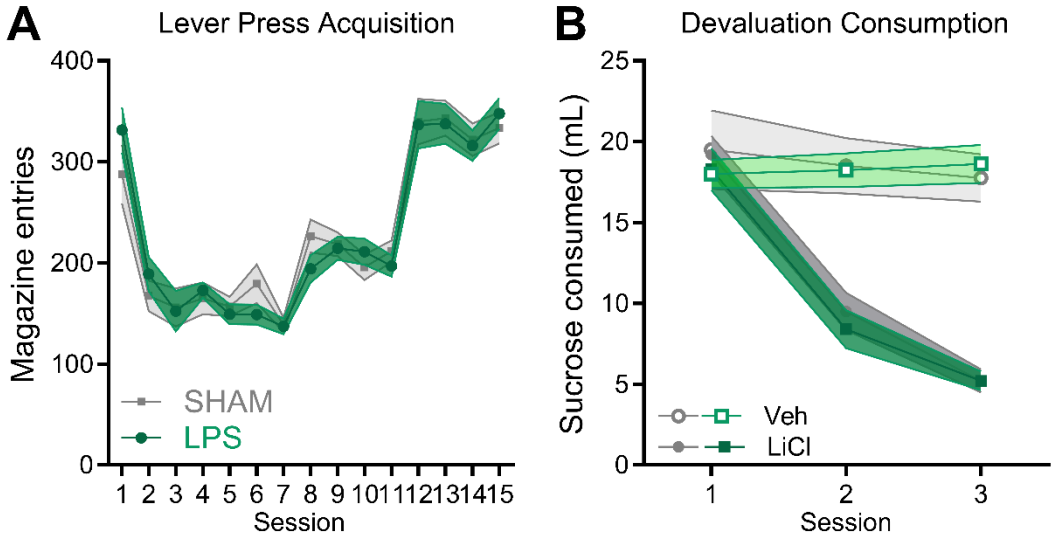

Supplemental Figure 2, relates to Figure 2. pDMS neuroinflammation did not alter magazine entries during lever press acquisition, nor sucrose devaluation by conditioned taste aversion. *(A) Magazine entries per min (±SEM) during instrumental conditioning, main effect of day F (14,546) = 51.27, p = 0.000, no Sham/LPS difference, F (1,39) = 0.002, p = 0.9629, and no day x group interaction, F < 1, (B) Millilitres of sucrose consumed (±SEM) during conditioned taste aversion training, session x devaluation interaction, F (1.64,60.9) = 90.44, p = 0.000 that did not interact with group, F < 1.*

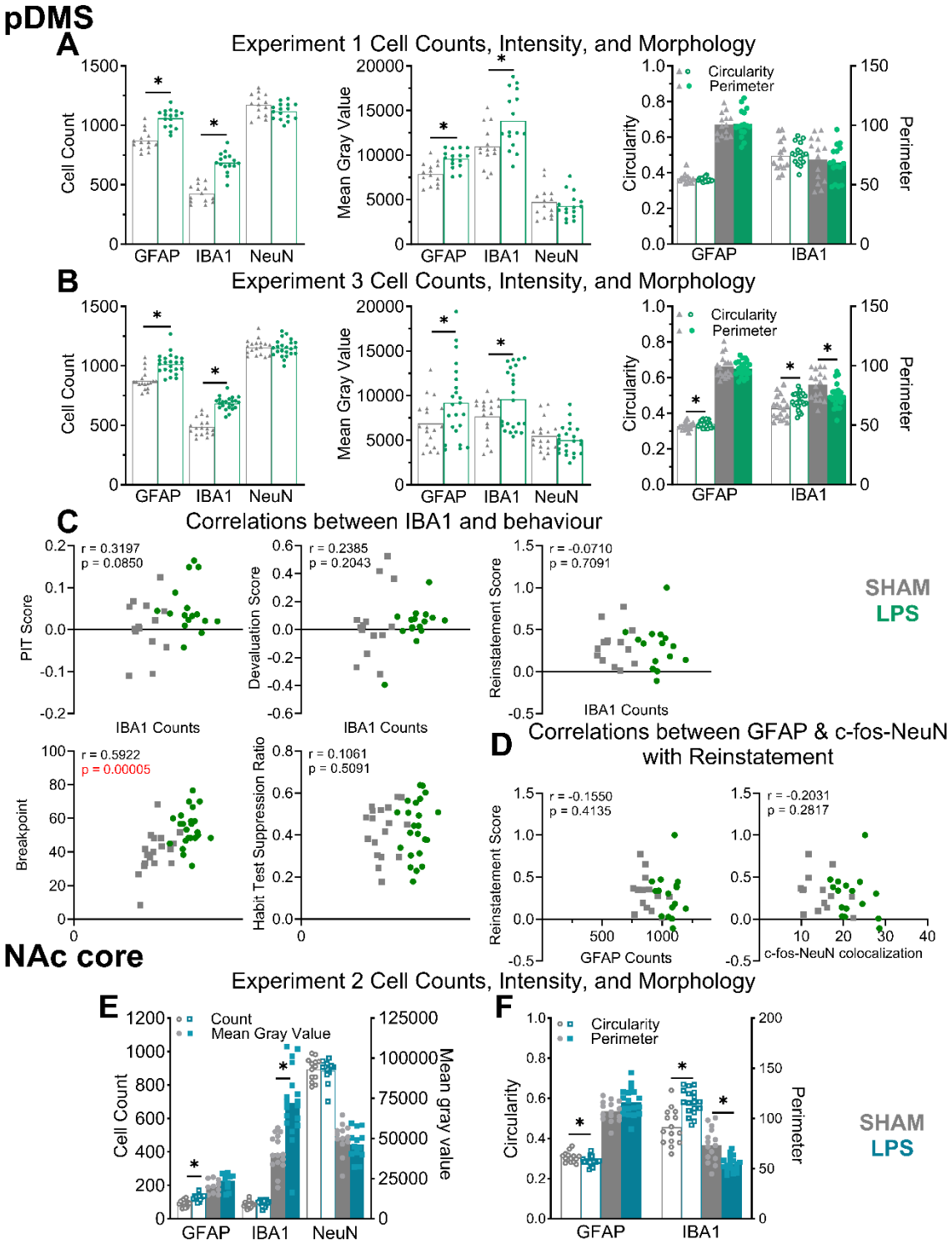

Supplemental Figure 3. Relates to Figure 3. Supplemental immunohistochemical results following injections of lipopolysaccharide (LPS) into posterior dorsomedial striatal (pDMS) in Experiments 1&3. *(A-B) Individual data points and mean values for quantification of, from left to right, cell counts, mean gray value, circularity (left y axis) and perimeter (right y axis) of GFAP, IBA1, and NeuN from rats in (A) Experiment 1 and (B) Experiment 3. For Experiment 1: cell counts were significantly higher in LPS tissue relative to Sham for GFAP, t(28) = 6.255, p = 0.000, and IBA1, t(28) = 8.74, p = 0.000, but not for NeuN, t(28) = 1.9, p = .068, mean gray*

*value was likewise significantly higher in LPS tissue relative to Shams for GFAP, $t(28) = 4.046$, $p = 0.0004$, IBA1, $t(28) = 2.799$, $p = 0.0092$, but not for NeuN, $t(28) = 0.7616$, $p = 0.4527$, circularity and perimeter of cells did not differ for any GFAP-positive or IBA1-positive cells in Experiment 1, closest $t(28) = 0.77$, $p = 0.443$, for IBA1 perimeter. For Experiment 3: cell counts were significantly higher in LPS tissue relative to Sham for GFAP, $t(39) = 5.38$, $p = 0.000$, and IBA1, $t(39) = 10.27$, $p = 0.000$, but not for NeuN, $t(39) = 0.336$, $p = 0.074$, mean gray value was likewise significantly higher in LPS tissue relative to Shams for GFAP, $t(39) = 2.072$, $p = 0.045$, IBA1, $t(39) = 2.088$, $p = 0.043$, but not for NeuN, $t(39) = 0.8789$, $p = 0.3848$, GFAP-positive cells were significantly more circular for this experiment, $t(39) = 2.152$, $p = 0.0378$, as were IBA1-positive cells, $t(39) = 2.109$, $p = 0.0414$, whereas perimeter of GFAP-positive cells did not differ between groups, $t(39) = 0.7562$, $p = 0.4541$, but was significantly lower in IBA1-positive cells for LPS animals, $t(39) = 2.665$, $p = 0.0113$. (C-D) Correlations between (C) IBA1, and (D) GFAP and c-fos-NeuN percentage colocalization and behavioural performances, r and p values displayed on graphs. (E-F) Results of analyses of immunohistochemical labelling of GFAP, IBA1, and NeuN following NAc core neuroinflammation, (E) Individual data points for cell counts (open shapes and left y axis) and Mean Gray Value (closed shapes and right y axis) values for GFAP (increased counts, $t(26) = 4.886$, $p = 0.000$, but not intensity, $t(26) = 0.3273$, IBA1 (increased intensity, $t(26) = 5.110$, $p = 0.000$, but not counts, $t(26) = 0.9705$, $p = 0.5238$, and NeuN-positive cells (did not differ between groups), (F) Individual data points for circularity (open shapes and left y axis) and perimeter (closed shapes and right y axis) for GFAP (significant decrease in GFAP circularity, $t(26) = 2.412$, $p = 0.047$; perimeter was unchanged, $t(26) = 1.955$, $p = 0.1209$) and IBA1 (significant increase in IBA1 circularity, $t(26) = 3.829$, $p = 0.0024$; significantly smaller perimeter, $t(26) = 3.502$, $p = 0.0055$). * denotes that the $p < 0.05$.*

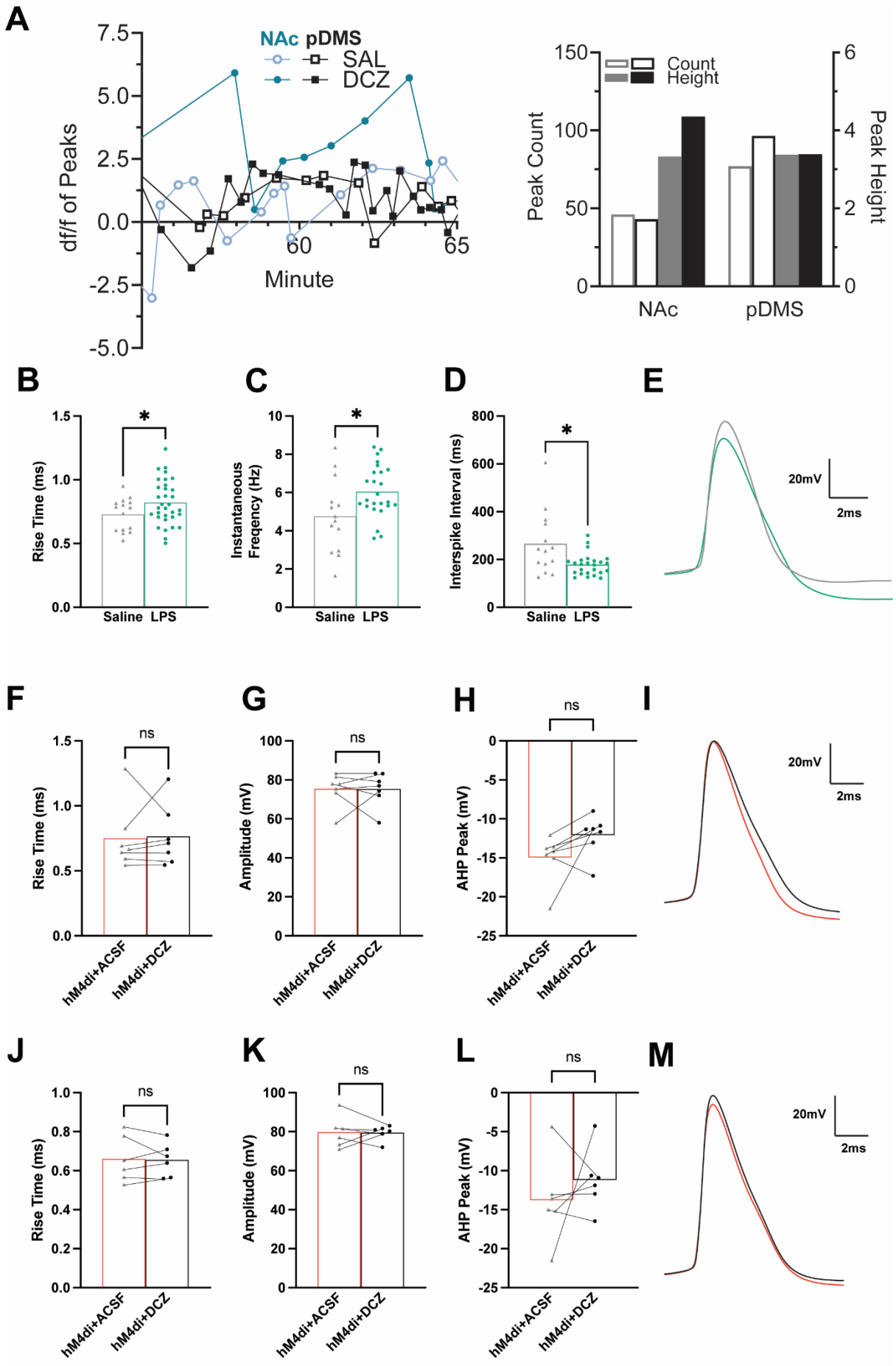
A
NAc pDMS
SAL
DCZ
df/f of Peaks
Minute
Count
Height
Peak Count
Peak Height
NAc
pDMS
B
C
D
E
Rise Time (ms)
Instantaneous Freqency (Hz)
Interspike Interval (ms)
Saline
LPS
20mV
2ms
F
G
H
I
J
K
L
M
ns
Amplitude (mV)
AHP Peak (mV)
hM4di+ACSF
hM4di+DCZ

Supplement Figure 4. Relates to Figure 4. *Supplemental data from fibre photometry (A) and whole-cell patch clamp electrophysiology recordings of MSNs following (B-E) LPS or sham injections into the pDMS or (F-I) following the application of hM4Di-DREADD agonist deschloroclozapine (DCZ) to transfected astrocytes. (B-D) Individual data points and means showing (B) increased rise time (t36.26 = 2.038, p = 0.0489), (C) increased instantaneous frequency (t20.47 = 2.245, p = 0.0359), and (D) reduced interspike interval (t16.23 = 2.417, p = 0.0278). Rise time changes are further reflected in (E) example cell average traces for the AP profile characteristics (LPS = green, saline = grey). Individual data points and means following DCZ application with MSNs at (F-I) RMP or (J-M) voltage clamped at -80mV. Data reflected in example cell profile traces presented in (I and M; ASCF = grey, DCZ = black) show AP profile characteristics of rise time and amplitude in the top traces and AHP profile in the bottom traces. LPS vs saline; LPS at RMP n = 33 cells and at -80 voltage clamp n = 32 cells, from n = 4 animals; saline; n = 15 cells from n = 3 animals. GFAP-HM4Di n = 7 cells from n = 2 animals tested with ACSF then DCZ.*

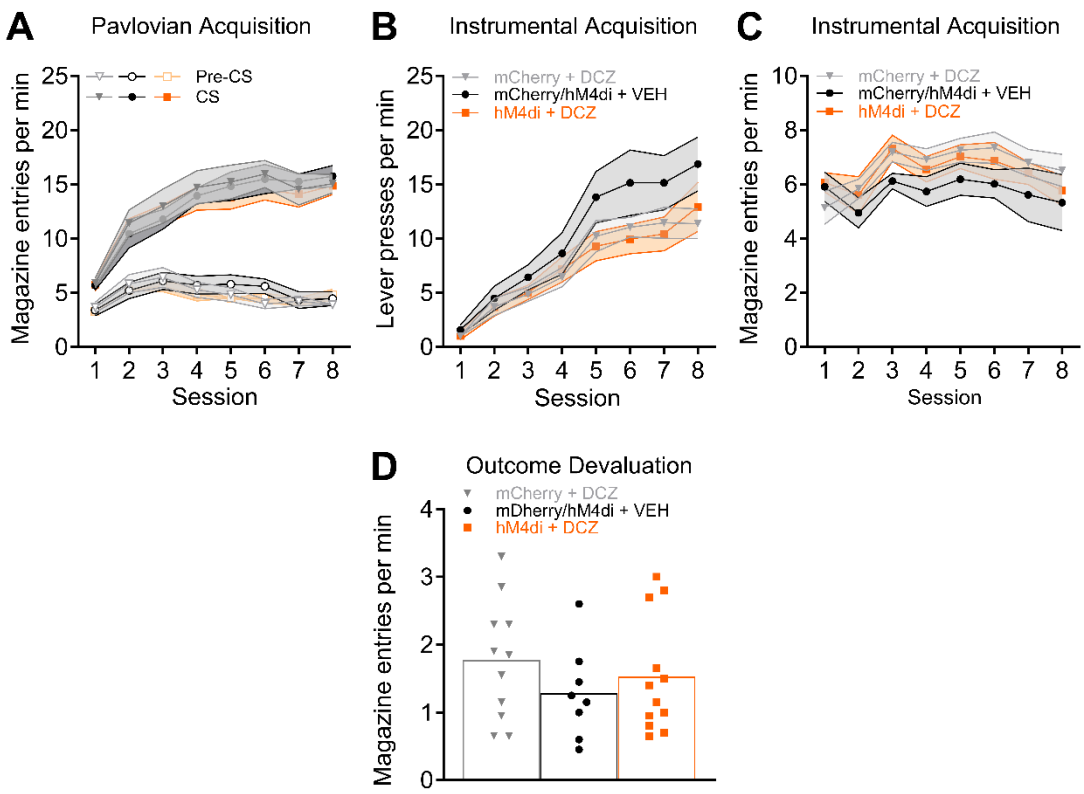

Supplemental Figure 5. Relates to Figure 5. Supplemental behavioural results. *(A) Magazine entries per min (±SEM) during Pavlovian conditioning, supported by a main effect of CS period (preCS vs CS) F (1,28) = 742.205, p = 0.000, and of Day F (7,196) = 27.685, p = 0.000, and a Day x CS period interaction (preCS vs CS) F (7,196) = 48.789, p = 0.000. No main effect of group or any interactions with group has been detected, Fs < 1, (B) Lever presses per min (±SEM) during instrumental conditioning, supported by a main effect of day F (7, 196) = 67.262, p = 0.000, no main effect of group (F (2, 28) = 1.803, p = 0.183) and no day x group interaction (F (14, 196) = 1.281, p = 0.222), largest F (5.66, 79.3) = 1.281, p = 0.277, for group x session interaction, (C) Magazine entries per min (±SEM) during instrumental conditioning, supported by a main effect of day F (7, 196) = 8.831, p = 0.000, no main effect of group (F (2, 28) = 1.827, p = 0.180) and no day x group interaction (F (14, 196) = 0.592, p = 0.870), largest F (10.18, 142.47) = 0.592, p = 0.821, for group x session interaction, (D) Individual data points and mean magazine entries per min during outcome devaluation testing, no group differences in magazine entries on test, F (2, 28) = 0.8223, p = 0.4497.*